AD-A035 747 NAVAL RESEARCH LAB WASHINGTON D C F/G 20/7
NRL VAN DE GRAAFF OPERATION, 1 JANUARY - 31 DECEMBER 1975.(U)
NOV 76 J W BUTLER
UNCLASSIFIED NRL-MR-3421 NL

1 OF 1
AD-A
035 747



END
DATE
FILMED
3-24-77
NTIS

U.S. DEPARTMENT OF COMMERCE
National Technical Information Service

AD-A035 747

NRL VAN DE GRAAFF OPERATION
1 JANUARY - 31 DECEMBER 1975

NAVAL RESEARCH LABORATORY
WASHINGTON, D.C.

NOVEMBER 1976

AD A035747

NRL Memorandum Report 3421

NRL Van de Graaff Operation 1 January - 31 December 1975

EDITED BY J. W. BUTLER

Ion Beam Applications Branch
Radiation Technology Division

November 1976

D D C
RECEIVED
FEB 18 1977
A

REPRODUCED BY
NATIONAL TECHNICAL
INFORMATION SERVICE
U. S. DEPARTMENT OF COMMERCE
SPRINGFIELD, VA. 22161

NAVAL RESEARCH LABORATORY
Washington, D.C.

Approved for public release; distribution unlimited.

SECURITY CLASSIFICATION OF THIS PAGE (When Data Entered)

REPORT DOCUMENTATION PAGE

READ INSTRUCTIONS BEFORE COMPLETING FORM

1. REPORT NUMBER: NRL Memorandum Report 3421	2. GOVT ACCESSION NO.
3. RECIPIENT'S CATALOG NUMBER	
4. TITLE (and Subtitle): NRL VAN DE GRAAFF OPERATION 1 JANUARY – 31 DECEMBER 1975	5. TYPE OF REPORT & PERIOD COVERED: Final report on an NRL problem.
	6. PERFORMING ORG. REPORT NUMBER
7. AUTHOR(s): J. W. Butler, editor	8. CONTRACT OR GRANT NUMBER(s)
9. PERFORMING ORGANIZATION NAME AND ADDRESS: Naval Research Laboratory, Washington, D.C. 20375	10. PROGRAM ELEMENT, PROJECT, TASK AREA & WORK UNIT NUMBERS: Program Element 61153N-11, 61153N-12, and 61153N-22; Cont'd
11. CONTROLLING OFFICE NAME AND ADDRESS: Department of the Navy, Office of Naval Research, Arlington, Virginia 22217	12. REPORT DATE: November 1976
	13. NUMBER OF PAGES: 75
14. MONITORING AGENCY NAME & ADDRESS (if different from Controlling Office)	15. SECURITY CLASS. (of this report): UNCLASSIFIED
	15a. DECLASSIFICATION/DOWNGRADING SCHEDULE

16. DISTRIBUTION STATEMENT (of this Report)

Approved for public release; distribution unlimited.

17. DISTRIBUTION STATEMENT (of the abstract entered in Block 20, if different from Report)

18. SUPPLEMENTARY NOTES

19. KEY WORDS (Continue on reverse side if necessary and identify by block number)

Van de Graaff accelerator
Ion implantation
Ion-induced x-rays
Ion optics
X-ray satellites
Solar cells
Nuclear analytical methods
Materials analysis

20. ABSTRACT (Continue on reverse side if necessary and identify by block number)

This document is the eleventh and final report of a series of summaries of the use and development of the NRL 5-MV Van de Graaff accelerator and associated equipment. The first six were semiannual summaries; and the next five (including the present one) were annual summaries. The present report includes a section on facility development and improvement, including specific reports on (i) the development of new species of ion beams from the Van de Graaff and (ii) the construction of a new 200-kV ion implantation system. A section on research highlights

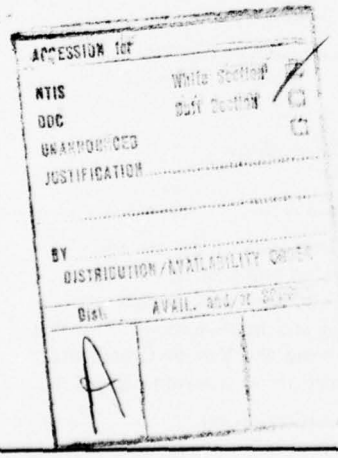
(Continues)

DD FORM 1 JAN 73 1473 EDITION OF 1 NOV 65 IS OBSOLETE
S/N 0102-014-6601

SECURITY CLASSIFICATION OF THIS PAGE (When Data Entered)

10. Program Element, Project, Task Area and Work Unit Numbers
Projects RR 001-09-41-5676, RR 012-06-41-5012, RR 022-08-44-5514;
Task Areas RR0110941, RR0120641, and RR0220844; and
Work Units 66H01-42, 66H01-44, and 66H01-43.

20. Abstract
includes descriptions of experiments on reactor material neutron damage simulation by heavy-ion bombardment, x-ray emission during bombardment of materials by heavy ions, materials modification by ion implantation, and materials analysis by ion beams. The final section includes brief descriptions of service irradiations for scientists outside the Branch.



CONTENTS

I. INTRODUCTION 1

II. VAN DE GRAAFF OPERATION 3

III. FACILITY IMPROVEMENT AND MAINTENANCE

A. Development of New Ion Beams 4
B. Reduction of Van de Graaff X-ray Loading 6
C. Telemetering System Troubleshooting 10
D. Measurements of Ion Source Beam at Van de Graaff Terminal 10
E. Curved-crystal X-ray Spectrometer 10
F. The 100-kV Ion-implantation Facility 11
G. New Ion-implantation System 12
H. The 200-kilovolt Power Supply 14

IV. RESEARCH HIGHLIGHTS

A. Ion-beam-simulation Irradiations 15
B. Cooperative Radiation Effects Simulation Program (CORES) Experiments 17
C. Modifications to the E-DEP-1 Computer Program 18
D. New Matrix Effect in Ion-excited X-ray Elemental Analysis 19
E. Chemical Effects in High-resolution X-ray Spectra 21
F. Ion-excited Vacuum Ultraviolet Spectral Studies 25
G. Photographic Image Enhancement by Ion-excited X Rays and Rutherford Backscattering 31
H. Measurements of Trace Quantities of Fluorine from Slip-ring Lubricant 35
I. Materials Analysis with the Magnetic Spectrometer 35
J. Techniques for Deep Profiling of Aluminum in Silicon-on-Aluminum-Oxide Structures by Means of the $^{27}Al(p,\alpha)^{24}Mg$ Reaction 41
K. Software for Nuclear Resonance Depth-concentration Profiles 42
L. The Treatment of Energy-loss Fluctuations in Surface-layer Analysis by Ion Beams 43
M. Reduction of Wear of Sliding Surfaces by Ion Implantation 47
N. Modification of Friction by Ion Implantation 53
O. Ion Implantation of Au Electrical Contacts 55
P. Ion Implantation in Superconducting Niobium Thin Films 55
Q. The Application of Pearson Distributions to Implanted Ion Profiles 57

V. SERVICE NOTES

A. Charged-particle Damage Study of Wrap-around Junction Solar Cells 60
B. Ion Implantation of Cu Laser Mirrors 62
C. Depth Profiling by Nuclear Resonance Method 63
D. Particle-channeling Investigation of Silicon Lattice Reordering 63
E. Nuclear Reaction Analysis of SiON Thin Films 64
F. Detection of Cl in SiO_2-Si Samples 64

VI. PUBLICATIONS AND TECHNICAL TALKS

A. Publications in Archival Journals 65
B. NRL Formal Reports and NRL Memorandum Reports 65
C. Talks Presented at Scientific Meetings 67
D. Miscellaneous Reports 68

NRL VAN DE GRAAFF OPERATION
1 January — 31 December 1975

I. INTRODUCTION

This document is the eleventh and final report of a series of summaries of the use and development of the NRL 5-MV Van de Graaff accelerator and associated equipment. The first six were semiannual summaries; and the next five (including the present one) were annual summaries. The series was started in 1968 by the Van de Graaff Branch, whose investigations were centered around the ion beams provided by the Van de Graaff accelerator. The scope of the operation reports gradually widened to include almost all of the work of the Branch.

In March 1975, the Branch was renamed the Ion Beam Applications Branch, whose organization as of 31 December 1975 was as follows.

6670 Ion Beam Applications Branch

J. W. Butler, Head
G. Moore (Secretary)
C. Taylor[1]

6671 Ion Irradiations Section

P. R. Malmberg
W. Lucke
C. Kennedy
J. Westmoreland
W. Young[2]
R. Corazzi
J. Herndon

6672 Materials Analysis Section

A. R. Knudson
J. Hirvonen
K. Burgart
K. Hill[3]

For the past few years the research effort of the Branch has been increasing in the area of materials modification by means of ion implantation. The present report includes descriptions of this research involving ion implantation as well as materials analysis by means of ion beams from the Van de Graaff accelerator. In addition, this report presents the vital operation statistics of the Van de Graaff accelerator, facility improvement and maintenance, research highlights, and service irradiation notes.

[1]Junior Fellow.
[2]Retired, intermittent status.
[3]NRC-NRL Postdoctoral Research Associate.

Note: Manuscript submitted November 12, 1976.

In March 1976 the Branches in the Radiation Technology Division were reorganized along program lines instead of facility lines so that in effect all Branches use whatever major facility serves the purpose at hand. For example, a single research project may use all three accelerators in different phases of the project. Hence it appears that facility operation reports no longer serve a useful function; therefore this report is the final one in the Van de Graaff series.

II. VAN DE GRAAFF OPERATION 1 January - 31 December 1975

(C. A. Kennedy)

A. Use/Maintenance

	Hours	Percentage of Total Time
1. Belt-on Time for Experiments	1146	73.51
2. Belt-on Time for Maintenance	22	1.41
3. Belt-off Maintenance Time	391	26.08
	1559	100.00

B. Staff/Other

	Hours	Percentage of Total Time
1. Branch Staff and Collaborators	1054	91.97
2. Service	92	8.03
	1146	100.00

III. FACILITY IMPROVEMENT AND MAINTENANCE

This section describes some of the significant facility improvements and maintenance activities during 1975. New ion beams have been produced in the Van de Graaff accelerator, and the construction of a new ion implantation system that will initially operate at about 200 kV with a beam of about 0.1 ma is almost complete.

A. Development of New Ion Beams (P. R. Malmberg, J. R. Herndon, J. K. Hirvonen, and W. H. Lucke

The various programs of the Ion Beam Applications Branch and collaborating groups require the availability of beams of ions of many different atomic species, both at high energies (Van de Graaff) and at lower energies. A continuing effort is being made both to obtain ion beams of additional elements and to utilize them for implantation and irradiations.

Three ion sources are currently in use: (1) An rf ion source for particles conveniently available in a gaseous form, (2) a modified Hill-Nelson sputtering type ion source for elements conveniently obtainable by sputtering, and (3) a hot-filament Colutron ion source. The first and second are used in the Van de Graaff, and the second and third are used on the 100-kilovolt ion implantation facility. The low-energy ion implantation system is used as an ion source test facility for both the Hill-Nelson and Colutron ion sources, and extensive use of it is made for actual implants as discussed in section III F.

In the modified Hill-Nelson ion source there are presently three arrangements for supporting the material to be sputtered. The method used depends mostly on the melting point and vapor pressure of the material to be sputtered. Since generally, more beam is obtained by running the sputtering element at a temperature approaching (but less than) its melting point, the three methods vary in the amount of cooling they provide to the sputtering material. For low-vapor-pressure elements and refractory metals a small piece of the element is used with a hole drilled in it and is supported by a 0.040-inch diameter tantalum wire through this hole. This provides minimum cooling and is used for elements such as molybdenum and chromium. For medium-range melting elements such as nickel and iron, the sputtering material is usually in the form of a cylinder turned down on one end and clamped in a hole in a supporting rod. This arrangement allows some cooling but not a great deal. Lower-melting-point materials are melted or pressed into the end of an internally cooled copper rod allowing a maximum amount of cooling.

Beams of four additional elements have been obtained on the test setup. Two of these, erbium and vanadium, used the first sputtering arrangement described. Erbium has a melting point in the middle range, but it was used in this manner due to limited quantity available, and

care had to be exercised to keep the source power low enough so that it would not melt. A current of 4.5 microamperes was measured for erbium, but this was under such poor resolution conditions that essentially all of the isotopes were included in the collected current. A beam of 440 nA was obtained of nearly monoisotopic vanadium.

A beam of tin was obtained with the internally cooled copper-rod method. Again the mass resolution was not ideal and permitted current collection from several isotopes, but a maximum current of 3.5 microamperes was obtained. This trial of tin was interesting in that tin has a relatively low melting point (232 ^{o}C), yet it was kept from melting (forced air was used for cooling). Higher-vapor-pressure elements such as tin could be readily used in sources with an oven; however there may be some advantages in use of the more readily controlled sputtering arrangement.

A 3-microampere beam of cadmium was obtained with the Colutron ion source. An oven arrangement was used to heat the cadmium, which was in metal form, to an adequate vapor pressure to be carried into the source by the argon supply gas. A cadmium beam had been obtained in 1973 with CdS in this source, but use of the metal is preferable.

In 1975, beams of the elements iron, molybdenum, silicon, and praseodymium were added to those used in the Van de Graaff, all four utilizing the modified Hill-Nelson source. All had been tested on the lower energy setup previously, although the prior test for praseodymium was only marginally satisfactory because the sputtering electrode arrangement was of an earlier, less satisfactory design.

Iron was used for three different sets of runs during the year; the arrangement was that of an iron cylinder clamped in a rod which in this case was also made of iron. In the first two sets of runs, beams of several microamperes were readily obtained, and there was no trouble. However, in the third set with conditions nominally the same the sputtering electrode melted twice before runs were initiated. Therefore a trial was made with the support rod and electrode constructed as one single piece of iron, and this seemed to work and was used; but there is still no satisfactory explanation of why this melting trouble suddenly occurred.

For molybdenum the tantalum wire arrangement was used. Since molybdenum is a refractory metal, its vapor pressure is low enough at the ion-source operating temperature that sputtered atoms stick to the walls instead of being reevaporated; hence the beam was lower than in the case of iron, for example. A beam of about 30 nA of $^{98}Mo^{+}$, the most abundant isotope (24%), was obtained. The source had to be run at high power, and the filament lifetime was thereby shortened.

The silicon was used in the form of a truncated conical slug pressed into the cone shaped end of an internally (water) cooled copper-rod support. A beam of $^{28}Si^{+}$ of 400 nanoamperes was obtained. However, the filament life turned out to be extremely short for reasons unknown, and the second of the two trials lasted only five hours. Unless means could be found to eliminate this difficulty, suitability of obtaining silicon beams in this manner is marginal.

The rare earth element, praseodymium, also used the cooled copper support rod. Praseodymium is monoisotopic, and a beam of one micro-ampere was obtained. Since praseodymium corrodes slowly in air, a means must be provided to protect it during the storage that occurs between uses.

Figure 1 is a nomograph that characterizes the variety of ion beams obtained from both the Van de Graaff accelerator and the low-energy ion implantation systems in terms of the atomic number Z of the accelerated ion and its output energy.

B. Reduction of Van de Graaff X-ray Loading (P. R. Malmberg, C. A. Kennedy, J. E. Westmoreland, J. R. Herndon, and J. K. Hirvonen)

When the modified Hill-Nelson ion source was first installed in the Van de Graaff accelerator, it was quickly apparent that x rays produced inside the Van de Graaff (as measured by an external Geiger-tube monitor) were considerably higher than with the rf ion source. These x rays are caused by backstreaming high-energy electrons that strike the accelerator tube near the upper end or strike material near the ion source. These backstreaming electrons are produced when the beam from the ion source, scattered by gas in the accelerator tube, strikes surfaces downstream in the accelerator tube or just beyond the end of it.

These electrons and the associated x rays have several deleterious effects. One such effect is the creation of a radiation health hazard. Although this problem is not serious, and can be minimized by roping off the hotter areas, people in other areas can still get some exposure; and in any case it is desirable to minimize x-ray exposures.

The second such effect is that these electrons and x rays degrade the performance of the Van de Graaff. The electrons cause additional ionization of the gas in the accelerator tube, and the x rays cause ionization in the high-pressure gas inside the Van de Graaff tank. These currents place an additional load on the charging system for the Van de Graaff terminal. But even more seriously, the various currents can cause potential distributions to be appreciably modified so that it is difficult to maintain a stable beam; or sparking may be promoted.

The principle reason for these higher x-ray levels with the Hill-Nelson ion source is that, because of the manner of its construction, the rate of gas flow out of the Hill-Nelson ion source is appreciably higher than that from the rf source. The gas from the rf source escapes from a long hole through a probe (which the beam also goes

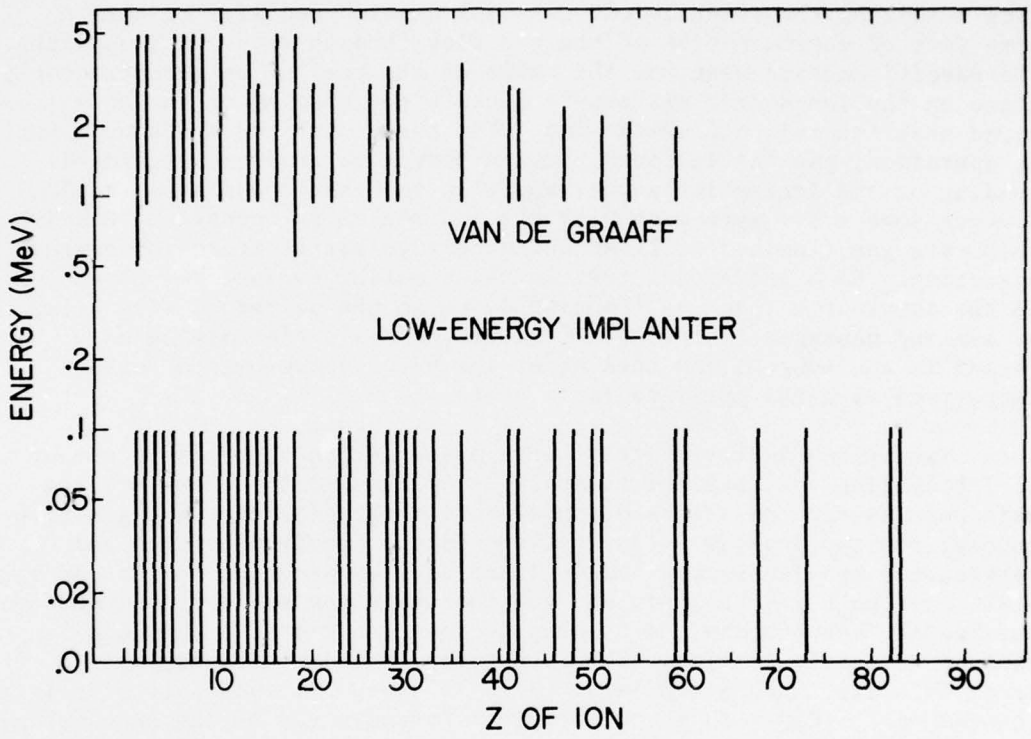


Fig. 1 — Energy range and atomic number of all the ion beams that have ever been implanted by the Branch implantation facilities

through); but in the case of the Hill-Nelson source the hole is in a thin graphite disc. The gas also can escape between this disc and a molybdenum cup supporting the disc and also between this molybdenum cup and the main ion source housing.

In December 1974 and continuing into January 1975, tests were made utilizing the 100-kilovolt ion implantation facility to obtain some sort of determination of the gas flow through these various paths. The specific measurement was the ratio of the reading on a thermocouple gauge on the ion-source gas supply line to the reading on an ionization gauge near the main diffusion pump. For tests with the ion source not in operation, gas was let into the ion source to produce a standard reading on the ionization gauge, and then the thermocouple was read. However some tests were made with the ion source in operation, and in this case gas flow had to be adjusted to give satisfactory ion source operation. Each individual test involved making an internal change in the ion source (such as changing discs to get different size holes or sealing passages by the use of vacuum grease), reobtaining a vacuum in the source, and then after the base vacuum became satisfactory to make the pressure-ratio tests.

Twenty-one different tests were made, and an appreciable amount of information was obtained by analysis of these data. However, the main results for the standard configuration were (a) that the gas flow through the two leakage paths (between disc and molybdenum cup and between cup and ion-source housing) are each about equal to that of a 0.020-inch hole in the disc, and (b) that when the source is run hot the leakage between cup and housing decreases because the hot cup expands to partially close the gap between it and the housing. Normally a disc with a 0.028-inch hole is used. If this hole size is changed to 0.020-inch the nickel beam (as measured on the test setup) is reduced by 1/3.

Nothing of course can be done about gas going out the hole in the disc. The leakage path between the cup and housing can be reduced somewhat by bridging this path with tantalum sheet fastened to the cup and housing; but this remedy has been only partially successful. The molybdenum cup normally has a hole in it considerably larger than the hole in the graphite disc; and since the leakage gas between disc and cup has to go out this hole, reducing the size of the hole in the molybdenum cup was expected to cut the leakage. Therefore a new molybdenum cup was made with a 0.046-inch center hole. A significant improvement was observed; in tests with the source cold and with a 0.028-inch hole in the disc the gas leakage was reduced 25%.

A relatively small reduction in gas leakage (e.g., the 25% noted above) might result in a substantial improvement in Van de Graaff operation. Therefore a test was made in the Van de Graaff accelerator with the modified molybdenum cup. Also a disc with a 0.020-inch hole was used instead of one with the usual 0.028-inch hole. The philosophy

here was that in some cases it may be worthwhile to exchange a smaller beam for better overall operation. Surprisingly, it was found that substantially the same beam could be obtained with the smaller hole. This result might be because with the larger hole the ion optics may be poorer so that the additional ion beam egressing from the hole is not effective. Observation of improvements is very subjective because, even under what is considered constant conditions, the x-ray levels may vary with time by a factor of two. However, at the 2.8-MV potential commonly used for nickel irradiations, the x-ray level with the modified cup was lower than previously, and it was possible to keep adequate nickel beam when voltage was raised to 3.6 MV and still have the x-ray level no higher than during some of the running at 2.8 MV.

Another approach to the problem of x-ray level radiation is not to interfere with the backstreaming electrons but to stop them in material that will produce fewer x rays than the material they normally hit. The first requirement for doing this is to determine where the electrons are hitting. In principle this can be done by measuring the x-ray levels near the ion source and then to use this information to deduce the x-ray source locations. Three attempts were made to measure these x-ray levels. The first was by placing thermoluminescent dosimeters at various locations near the ion source and in the high-voltage terminal. The other attempts involved x-ray film, one with multiple films with lead absorbers in between. The results were consistent with the assumption that most of the electrons hit the various electrode and electrode support structures (not the accelerator tube electrodes) near the ion source and near the axis. Most of the material in this area is stainless steel although the holes along the axis were partially lined with thin aluminum alloy.

The decision was made to put graphite at all practical places where the more intense electron beams may strike. Therefore the liners were changed from aluminum to graphite and made as thick as possible without interfering with the beam; and liner material was extended up into the accelerator electrode. Also a massive flat disc of graphite was put on the large stainless steel support piece where it would face the electrons. The graphite pieces were outgassed in a vacuum furnace before first use. The Van de Graaff was then run with the carbon pieces installed. The general indication was that the x-ray level at 2.8 MV was reduced to 2/3 the level of the system without use of the graphite pieces, and that operation at 3.5 MV would be feasible.

The graphite pieces are now routinely used with the Hill-Nelson source operation. Combining this use with use of the modified molybdenum cup (which has not been used since the initial test) may make a substantial overall improvement.

C. Telemetering System Troubleshooting (C. A. Kennedy)

Tests have been made in an effort to locate the cause of random erratic operation in the telemetering system. There appear to be stray pulses at the input to the telemetering receiver whenever the erratic operation is present. There does not appear to be any problem when the accelerator is open and working off the house 400-Hz generator or when the accelerator is closed and operating off the internal 400-Hz generator as long as the terminal voltage is below about 0.7 MV. As the accelerator potential is increased above this point the frequency of recurrence of the problem in the system increases until a potential of about 1 MV is reached; above 1 MV the rate is relatively constant.

It is possible that the trouble is due to strong light pulses resulting from corona discharge on the structure. In order to check this possibility an optical collimating shield was placed on the detector. The installation of the shield has had no noticeable effect on the noise problem. Further investigations will be made into the source of this noise.

D. Measurements of Ion Source Beam at Van de Graaff Terminal (C. A. Kennedy)

An ion-source test feature has been installed in the terminal to facilitate monitoring at the console the total beam extracted from the ion source during test operation with the tank off. The amount of total beam current that can be extracted and focused through the input aperture of the accelerator lens is a good measure of the condition of the ion source.

This measurement is accomplished by disabling the accelerator lens power supply to ensure safe operation while the tank is off and connecting the second electrode of the accelerator lens to one channel of the telemetering system calibrated to measure the beam current collected at the lens. This provides a complete check of all ion source parameters up to the accelerator lens.

E. Curved-crystal X-ray Spectrometer (K. Q. Burgart)

A new vacuum chamber for the eleven-inch curved-crystal x-ray spectrometer has been designed, constructed, and tested. Improvements include an external stepping motor driving the crystal holder through a rotating vacuum seal. With rigid coupling and negligible backlash in the system, an improvement in reproducibility of data was obtained. An external control for adjusting the crystal angle is also included. The electronics for operating the driving mechanism provide either local manual control or remote computer control.

F. The 100-kV Ion-Implantation Facility (W. H. Lucke)

During 1975, the 100-kV ion implantation system was used to implant the ions of 13 atomic species, ranging from He to Bi, into substrates ranging from insulators to bearing steels. Energies have ranged from 2 to 80 keV; and fluences from 10^{10} to 10^{18} atoms per cm^2.

Most of the implantations were made in a straightforward manner, but the low-energy implantations were troublesome and tedious. This problem resulted from the fact that both beam intensity and optical quality are severely degraded at the lower energies (15 keV or less). For energies less than about 8 keV the loss in beam intensity was so great that it was necessary to apply a decelerating potential to the target chamber rather than to operate at such low accelerating voltages. This procedure required the insertion of a large aperture lens just ahead of the target chamber. The amount of deceleration that could be used however was limited by the distortion introduced by the lens, which has the effect of introducing uncertainties in the uniformity of the implanted fluence.

Another approach to the problems of low-energy operation was the installation of a strong focusing pair downstream from the analyzing magnet. Whereas preliminary trials gave an increase in beam intensity by a factor of 3 or 4, the optical quality appeared to be degraded. This difficulty might have been overcome by a careful determination of the optimum voltage to be applied to each element of the strong focusing pair; but for various reasons, including a great demand for machine time to do higher energy implants and the near completion of the 200-kV apparatus, this determination was never undertaken.

The only service implantations made in 1975 were 10- and 20-keV Na into SiO_2-on-Si substrates. These were done as part of a study of the effect of Na on MOSFET operation and reliability, funded by H. L. Hughes of the Electronics Division. An incident which occurred in the course of this work illustrated the effectiveness of secondary electrons in the neutralization of charge buildup in an implanted insulator. (These secondary electrons are ejected from metals adjacent to the implanted area by the incident beam.) For some of the 10-keV implantations the aluminum foil mask customarily used to outline the area of implanted ions, was inadvertently left off. Subsequent analysis showed very little Na present, and most of that which was found was not in regions exposed to the beam. Since sodium is known to be extremely mobile in SiO_2 in the presence of an electric field, it seemed clear that charge buildup was the cause of this peculiar behavior. The implantations were repeated with careful attention to the presence of masking Al foil. (A search of the literature revealed that Al was a prolific emitter of secondary electrons.) The analysis of these implants showed the expected amounts of Na in the implanted area and none elsewhere, a clear illustration of the usefulness of the masking technique.

G. New Ion-implantation System (P. R. Malmberg, C. A. Kennedy, R. J. Corazzi, J. R. Herndon, and J. K. Hirvonen)

The 100-kV ion implantation facility is an interim system while a new research-type ion-implantation system is designed and built. In late 1974 it became obvious that certain compromises between versatility and costs would have to be taken if the system were to be finished with the funds available at present. One particular decision was to use a spare section of the Van de Graaff accelerator tube as the accelerator tube for this facility for the immediate future. Another was to transfer the implantation beam leg from the 100-kV system to the new system and use it with only minor modifications.

The analyzing magnet to be used with the new system has a 24-inch-diameter poleface and weighs about 8 tons. Special support for this heavy magnet was required. Therefore steel plates to distribute the load over the concrete floor were installed. The magnet stand and analyzing magnet have been placed in position and aligned relative to both the 73° beam line from the Van de Graaff and the ion implantation high-voltage table. Subsequent transit checks of magnet position indicate that there is no settling, indicating the load distributing scheme is adequate. The magnet reversing switch and a double-throw switch to select either of two magnet power supplies have been installed with safety interlocks.

The ion-optical-ray tracing program LEIMRT, which had been developed for the SEL 840A computer, was used to make final selection of beam-line elements and, particularly, positions of elements along the beam path. The portion between the ion source and analyzing magnet was designed in late 1974; the implantation leg portion was designed this year. The general design involves an ion-beam crossover point between the accelerator tube and magnet, a strong focusing lens element (defocusing in horizontal direction) to adjust the beam to minimum horizontal dimension at the analyzing slit after the magnet, a drift section between this analyzer slit and a strong focusing quadrupole pair, scanner plates, and then a drift section before the target. Because a quadrupole pair already on hand will be used at first, the spot on target will not be as small and the maximum beam current may not be as big as it would be if a strong focusing lens of larger aperture were used.

The analyzing magnet is used with a wide gap (3 1/8 inches). A large vacuum chamber was completed in 1974 to make full use of this gap size. In 1975, flanges for all the port openings were made. Two of these flanges connect to tubing as part of the beam path; and another one has a tube projecting inside the chamber so that a Hall probe can be inserted to measure the magnetic field.

Although the top and bottom plates are of 3/8-inch stainless steel and should sag only slightly when the chamber is evacuated, additional support is given internally by 3/8-inch stainless steel posts, judiciously placed so that they would not interfere with expected beam paths. Since stray beams (other mass spots, molecular beams, etc.) of significant power could hit these posts, the tube for the Hall probe, or the aluminum side walls of the chamber, the most likely regions were covered with tantalum sheet, in general spaced away from the protected material so that the tantalum itself could get hot and dissipate its heat without getting nearby material too hot.

This magnet chamber was assembled and vacuum tested in December and installed in its final location in the magnet just before year's end.

A vacuum system utilizing a 6-inch diffusion pump is installed near the ground end of the accelerating tube, and a vacuum system utilizing a 4-inch diffusion pump is installed between the magnet and analyzer-slit section. (The implantation beam leg to be transferred has its own 4-inch diffusion pump vacuum system.) The 6-inch vacuum system was mounted on a metal angle framework; this framework also supports some beam-path components. The 4-inch vacuum system was mounted on a heavy welded assembly fastened to the magnet stand; this assembly also supports the analyzer-slit section. Each of these two vacuum systems terminates at the top in a cross; the horizontal direction of this cross forms part of the beam path.

The forepump-line systems were constructed, including valves, gauges, traps, and provision for roughing out the high-vacuum sections. Also vacuum control systems were constructed and checked out.

As previously mentioned, one of the short sections of the spare Van de Graaff accelerating tube is being used as the accelerating tube for this low-energy ion-implantation system. The accelerating tube has been mounted, connected to the main high-vacuum system, and aligned on the design beam line between ion source and analyzing magnet. An insulated column to give support from the floor has been constructed and installed at the high-voltage end of the accelerating tube.

Although a number of standard elements or elements on hand were used in the beam path, it was necessary to design and construct a number of elements and support structures. This was done for the path before the magnet, and this portion is now assembled. However, several of the elements beyond the magnet are yet to be designed and constructed, including the modifications to the old implantation beam leg that will be transferred.

The A. C. power system was designed by Public Works and installation started. This installation provides power for the analyzing-magnet power supplies, the vacuum pumping stations, the high-voltage power supplies, the isolation transformers, and the operating console.

The regulator amplifier and the reference power supply for the 600-amp power supply for the analyzer magnet have been rebuilt in order to consolidate the equipment. This is now mounted in the main power supply enclosure instead of a separate rack. A 250-amp power supply will be used at lower currents.

Work has continued on equipment installation on the insulated table for the ion source. Power supplies have been mounted and mechanical control linkages installed. Cables for power from the secondaries of the 115-V, 60-hz isolation transformers (one 3-KVA and one 6-KVA) have been run to the table; and 60-hz power distribution has been installed. The circulating pump and radiator for the ion-source cooling water has been installed.

The table shorting device and interlock for high-voltage supplies on the table is in place and operational. The panel containing cradles to hold lecture-size bottles for the ion source has been completed and is in place on the table. This system includes a dedicated valved line to be used for corrosive gases.

A resistor chain assembly made up of stacked anticorona discs having a pitch to match the accelerating tube has been designed. Resistors and anticorona discs have been received, and associated mechanical parts fabrication has been started. The resistor chain will have provisions for shorting individual sections as a means of altering the gradient along the accelerating tube and for controlling the voltage across a separate focusing section in order to focus the beam of accelerated particles.

H. The 200-kilovolt Power Supply (K. Q. Burgart)

The 200-kV power supply has been redesigned and rebuilt. Previously this supply had very poor regulation together with a very high output ripple (about 1% of the output voltage). There was also a continuous increase in the output voltage with time for constant settings.

Since it was desirable to continue to use as many of the original high-voltage components as possible, the original HV transformer, rectifiers, and filter capacitors were reused. The high-voltage-insulated transformer for the filament and other low-voltage power supplies was rewound with design changes. New amplifier circuit boards were constructed and redesigned, stable reference supply and low-voltage power supplies were included. The output high-voltage amplifier has been redesigned mechanically for better heat transfer and also incorporates new corona shields and sockets.

IV. RESEARCH HIGHLIGHTS

This section describes the research efforts during 1975. The first three reports involve the use of ion beams to simulate neutron radiation damage to reactor materials. The next four contributions involve spectrum measurements of x-rays emitted by solid materials under heavy-ion bombardment. The next five items involve materials analysis by means of "light-ion" beams (protons, deuterons, or alpha particles). The last five discussions involve the use of ion implantation in materials modification.

A. Ion-beam-simulation Irradiations (J. E. Westmoreland)

An extensive program of the Ion Beam Applications Branch in cooperation with other groups both within NRL and in other government laboratories and industry is the use of beams of heavy ions to simulate radiation effects for the study of potential reactor materials. In 1975, irradiations were performed with 2.8-MeV $^{56}Fe^{+}$, 2.8-MeV $^{58}Ni^{+}$, and 2.7-MeV $^{98}Mo^{+}$ ion beams. The variables for each particular case are listed below.

High-dose-rate (HDR) nickel-ion and iron-ion irradiations were performed with beams such as to give 7×10^{-2} displacements per atom per sec (dpa/sec). Low-dose-rate (LDR) nickel-ion irradiations were performed with a beam such as to give 7×10^{-4} dpa/sec. Some nickel-ion irradiations were also performed with an intermediate dose rate (IDR) producing a displacement rate of about 1.9×10^{-2} dpa/sec so that the results obtained from these samples could be directly compared with those of other laboratories as this was the purpose of this experiment. Molybdenum ion irradiations were performed with the maximum $^{98}Mo^{+}$ beam obtainable, which was equivalent to a damage dose rate of about 2.5×10^{-3} dpa/sec.

2.8-MeV $^{56}Fe^{+}$

Two commercial alloys of the ferritic class HT-9 and EM-12 (10-12 at. % Cr with additions of Mo, Nb, W, or Ta to provide solid solution hardening and more stable alloy carbides at high temperatures) have some promise for duct and cladding applications for advanced reactor concepts because of their favorable neutron absorption cross-sections. These two have been selected for study in the National Alloy Development Program. Seven samples of EM-12 and thirteen samples of HT-9 were irradiated in 1975, typically at temperatures from 450 to 650 ^{o}C and fluences equivalent to 40 to 250 dpa (contract work funded by ERDA).

2.8-MeV $^{58}Ni^{+}$

Various materials were irradiated in 1975 with 2.8-MeV $^{58}Ni^{+}$ ions as part of efforts on five separate experiments on related materials in the general area of understanding irradiation effects which impact on the general area of void swelling in reactor materials.

Fluence Dependence

In continuing work on the fluence dependence of swelling in pure Ni, nine samples were irradiated in 1975 to fluences from 1.3 to 130 dpa and at temperatures of 525, 575, and 625 ^{o}C.

Alloy Development Intercorrelation Program (ADIP)

Since the microstructures of most commercial alloys are complex, it is useful to study the mechanisms of void induced swelling basic to the austenite lattice with high-purity model systems, such as the Fe-Ni-Cr ternary alloys. The present experiment was performed as part of the ADIP program, an interlaboratory comparison of the void swelling produced by fast neutrons and a variety of charged particles. The alloy chosen for this experiment was nominally Fe-25 wt. percent Ni-15 wt. percent Cr. Twenty samples of this material were irradiated in 1975, all at the IDR, at temperatures from 600 to 750 ^{o}C and fluences from 10 to 90 dpa.

Dilute Solution Binary Nickel Alloys

In an effort to understand the mechanisms by which dilute solid solution additions are effective in reducing swelling, nine binary alloy samples were irradiated in 1975, all at fluences of 13 dpa and at temperatures ranging from 425 to 625 ^{o}C. The compositions were Ni-1 at. % W, Ni-1 at. % Co, Ni-1 at. % Cr, Ni-1 at. % Ti, and Ni-1 at. % Si.

Ni-Al Alloys: Temperature and Fluence Dependence of Void Swelling

As a model for the precipitate hardened commercial alloys, the Ni-Al alloy system was chosen. Two compositions were picked, Ni-6 at. % Al, a solid solution material, and Ni-14 at. % Al, where thermal aging after solution treating produced a convenient and suitable distribution of Ni_3Al precipitates of mean size about 400 Å. These precipitates are representative, for example, of the precipitates $Ni_3(Al,Ti)$ responsible for the precipitate hardening in the Nimonic series of alloys. Five samples of Ni-6 at. % Al were irradiated at temperatures from 575 to 625 ^{o}C and fluences from 6 to 200 dpa. Eight samples of Ni-14 at. % Al were irradiated at temperatures from 525 to 725 ^{o}C and fluences from 7 to 200 dpa.

Ni-Al Alloys: Dose-rate Effects on Precipitate Structure

Significant dose-rate effects have been seen previously on the void swelling in pure Ni. Several possibilities have been proposed for the behavior of precipitates under heavy-ion irradiation and their effects on void swelling. An investigation of these phenomena was continued with Ni-14 at. % Al alloy samples with precipitate structures as described above. Five HDR samples were irradiated, all at 725 ^{o}C, to fluences from 0.13 to 13 dpa. Four LDR samples were irradiated, all at 725 ^{o}C, to fluences from 1.3 to 13 dpa.

2.7-MeV $^{98}Mo^{+}$

Refractory materials have some promise for use in future advanced reactors where operating temperatures could exceed the acceptable values for the stainless steels. Five molybdenum samples were irradiated, one each of the temperatures 800 °C and 900 °C to a fluence of 2 dpa, one at a temperature of 800 °C to a fluence of 20 dpa, and two at a temperature of 900 °C to a fluence of 20 dpa (contract work funded by ERDA).

B. Cooperative Radiation Effects Simulation Program (CORES) Experiments (J. E. Westmoreland)

The primary research involvement of the Ion Beam Applications Branch in the CORES program in 1975 was in the area of dose rate-effects on precipitates in the Ni-14 at. % Al alloy system. This system is related to practical alloys but is simpler to study. The precipitates produce alloy hardening, and from the point of view of reactor materials it is important to ascertain the effects of radiation on such aspects as hardening as well as the more obvious aspect of swelling due to the production of voids. The rate of damage production is 3 to 5 orders of magnitude higher with heavy-ion simulation experiments than with irradiations with reactor neutrons; hence the effect of dose rate on the radiation effects must be measured and understood. It is possible to vary the dose rate by two orders of magnitude in the simulation experiments; results obtained here will aid in extrapolation to the reactor case.

As the CORES program has progressed it has become clear that the rate-limiting step in obtaining data was the transmission electron microscopy (TEM), not irradiation time on the Van de Graaff accelerator. Therefore a large part of Westmoreland's time was spent in 1975 continuing learning TEM, improving his TEM technique, and learning aspects of contrast theory necessary to properly interpret the images produced by TEM. It had been envisioned that this interpretation would be relatively straightforward, as is the case in unirradiated samples. However, it has turned out that this is not the case for heavily irradiated material of this class of alloys. At the end of 1975 there was still disagreement between investigators in this field as to the interpretation of certain resulting data.

So called "front face thinning" is the electropolishing of the irradiated surface of the sample to remove about 3500 to 4000 Å of the surface to expose the peak damage region created in the sample by the 2.8-MeV $^{58}Ni^{+}$ irradiation. Sufficient difficulty was experienced with the Ni-14 at. % alloy that the initial set of 13 and 1.3 dpa HDR and LDR samples was lost because the sample front face was inadvertently electropolished to such a depth that the entire damage zone was essentially removed. This shortcoming has been corrected by determining the

actual depth of one or more shallower "front face thinnings" on each sample by subsequent interference microscopy measurements of the step (or steps) at the edge of an area of the front face masked to prevent material removal in that area.

The data obtained to date show no appreciable dose-rate effect at 725 ^{o}C for fluences of 1.3 dpa. Indications of a change in the precipitate size distribution at 4 dpa have been seen, but the significance of this is not yet clear. Further insight is being gained at present through the study of the 13-dpa samples.

C. Modifications to the E-DEP-1 Computer Program (G. P. Mueller* and J. E. Westmoreland)

Two modifications to the 5 May 1973 version of the computer program E-DEP-1 were implemented in 1975.

The first modification[1] was specifically to enable the calculation of the energy deposition of high-energy helium ions in nickel and type-316 stainless steel. As an example, calculations for 70-MeV He incident on Ni and on type-316 stainless steel were performed, and the resulting output included as part of reference 1. This effort provided the values needed to aid in the design of a joint Radiation Technology Division and Engineering Materials Division experiment to simulate radiation induced creep in reactor materials by helium ion bombardment.

The second modification[2] was of a more general nature to allow any user, according to his specific needs, to calculate the energy deposition of higher-energy ions in amorphous solids. The original E-DEP-1 code is limited in beam energy by the form of the inelastic stopping law that it uses and by certain structural characteristics of the code. Other stopping laws are easily substituted; a sample is included in reference 2. The main body of reference 2 outlines the structural changes that are necessary in order to use E-DEP-1 for higher beam energies.

---

*Radiation Technology Division, Naval Research Laboratory.

[1]G. P. Mueller and J. E. Westmoreland, NRL Memorandum Report 3019, March 1975.

[2]G. P. Mueller and J. E. Westmoreland, NRL Memorandum Report 3194, January 1976.

D. New Matrix Effect in Ion-excited X-ray Elemental Analysis (K. W. Hill,* A. R. Knudson, and J. Comas†)

The use of ion beams to excite characteristic x rays has found broad applicability to materials analysis problems. Proton and helium beams are most generally used, but heavier ions have also been found to be useful in special situations. In thick samples the matrix effects, which have been observed with x-ray fluorescence analysis, will also occur with ion excitation; but we have observed an additional matrix effect in the case of heavy-ion excitation. In the present work it has been found that, over a substantial range of bombarding energies, a 50 at. % Al, 50 at. % Ti target (Al-Ti) is a more intense emitter of Al K x rays than a pure Al target when both are bombarded by energetic Ar ions. This lack of proportionality between the amount of an element present in the sample and the number of characteristic x rays emitted by that element has also been seen for Al-Fe and Al-Ni alloy targets and is expected to occur whenever the excitation mechanism is a two-step process involving, first, the creation of an electron vacancy in some shell of the projectile and, second, the transfer of that vacancy to an inner shell of a target atom with resultant x-ray emission. This excitation process was initially studied by Macek, Cairns, and Briggs.[1] The lack of proportionality occurs because of the widely varying efficiencies of different elements in producing the initial electronic vacancy in the projectile ion.[2]

X-ray yields from thick Al and Al-Ti targets were measured under bombardment by Ar ions in the energy region from 100 keV to 3.0 MeV by using a Si(Li) detector of 180-eV resolution (FWHM) to detect the Al K x rays. The measured thick target x-ray yields are shown in Figure 2. Our data for the pure Al target are in good agreement with the results of Taulbjerg et al.[3] in the region of overlap. Over the energy region from about 0.26 MeV to 1.25 MeV the Al K x-ray yield from the Al-Ti target actually exceeds that from the pure Al target. The ratio of the yields reaches a maximum value of 1.5 at approximately 500 keV. Throughout the energy region which was studied, the ratio of the yield from the Al-Ti target to the yield from the pure Al target exceeds the value of 0.5, which would be expected on the basis of target composition. (Actually, taking into account the higher average atomic stopping power and the higher self-absorption for Al K x rays in the Al-Ti target, one would expect this ratio to be somewhat less than 0.5.)

*NRC-NRL Postdoctoral Research Associate.
†Electronics Division, Naval Research Laboratory.
[1]J. Macek, J. A. Cairns, and J. S. Briggs, Phys. Rev. Lett. 28, 1298 (1972).
[2]F. W. Saris and D. J. Bierman, Phys. Lett. 35A, 199 (1971).
[3]K. Taulbjerg, B. Fastrup, and E. Laegsgaard, Phys. Rev. A8, 1814 (1973).

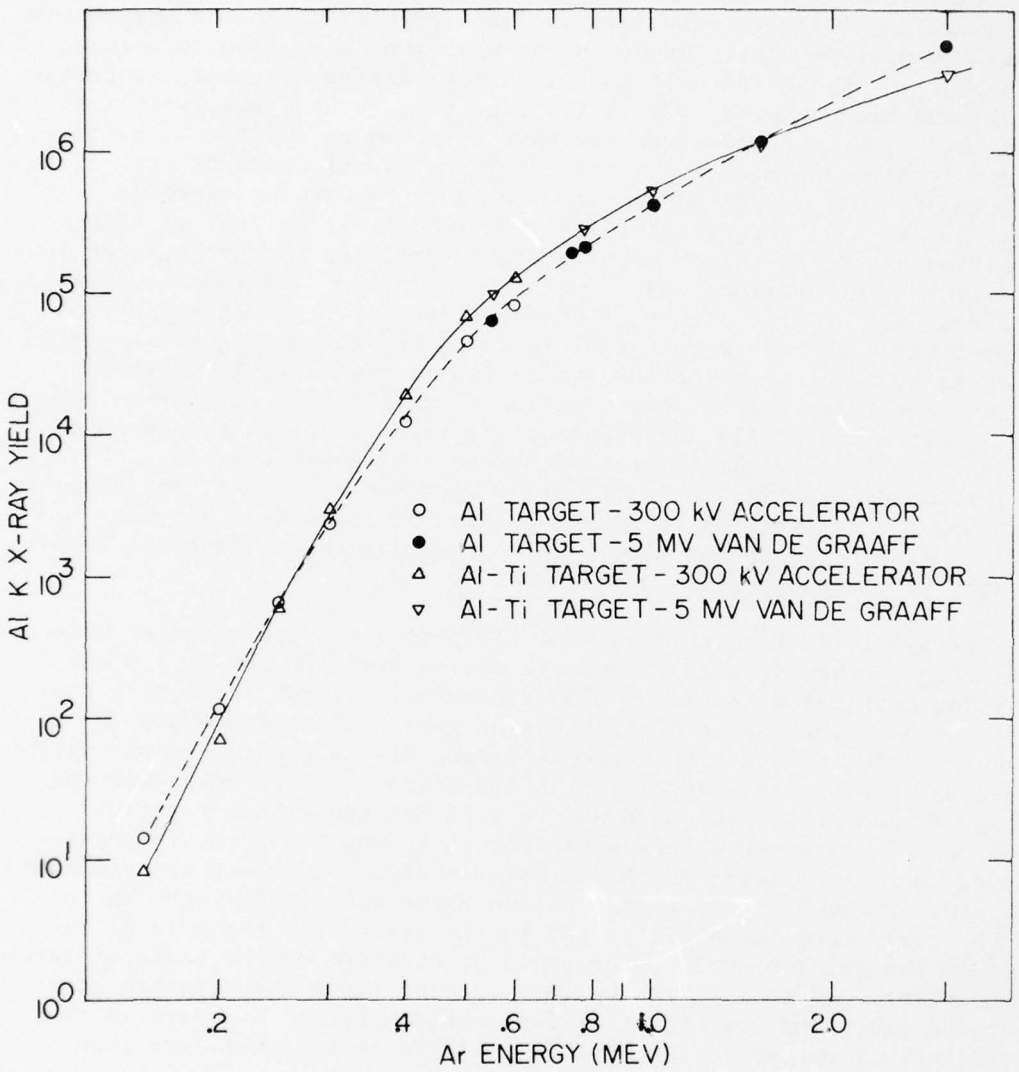


Fig. 2 — Al K x-ray yields from thick Al and 50 at. % Al, 50 at. % Ti targets bombarded by Ar ions

In order to remove the effects of target self-absorption and different stopping powers in the two targets we have applied the formula from Merzbacher and Lewis[4] to extract Al K x-ray production "cross sections" from these thick-target yields. Although this procedure is not valid for obtaining cross sections for two-step excitation mechanisms, such as recoil or Ar L-shell vacancy transfer to the Al K shell, in the present analysis the "cross section" is looked upon as just a proportionality factor relating the number of Al K x rays produced at a given energy to the number of Al atoms seen by the projectile while in an energy interval ΔE about the energy E. Since the projectile range is in all cases large with respect to the distance required to obtain equilibrium in the number of Ar L-shell vacancies, we believe that this is a valid approach. The ratios of the cross sections obtained in this manner are shown in Figure 3.

The minimum value of the cross-section ratio is consistent with an extrapolation of Saris' low-energy data,[2] which indicate that Al is about 1/10 as effective as Ti in producing Ar L-shell vacancies. The rise in the curve of Figure 2 at low energies is due to the decreasing importance of Ar L-shell vacancy transfer and the increasing importance of recoil in producing K-shell vacancies. At higher energies the superiority of Ti with respect to Al in producing Ar L vacancies probably decreases, and other mechanisms may be contributing to increase the cross-section ratio.

These results indicate that substantial care must be exercised in interpreting the results when heavy-ion excitation is used for elemental analysis.

E. Chemical Effects in High-resolution X-ray Spectra (K. W. Hill* and A. R. Knudson)

A chemical effect has been observed in the excitation of Al target x rays by ion impact. Such an effect is characterized by a dependence of the x-ray production cross section upon the chemical or solid-state environment of the emitting atom. These measurements might provide new information relative to transition probabilities for interatomic processes as well as providing information on collisional ionization processes.

---

[4]E. Merzbacher and H. W. Lewis, Encyclopedia of Physics, edited by S. Flugge (Springer-Verlag, Berlin, 1958), Vol. 34, p. 166.

*NRC-NRL Postdoctoral Research Associate.

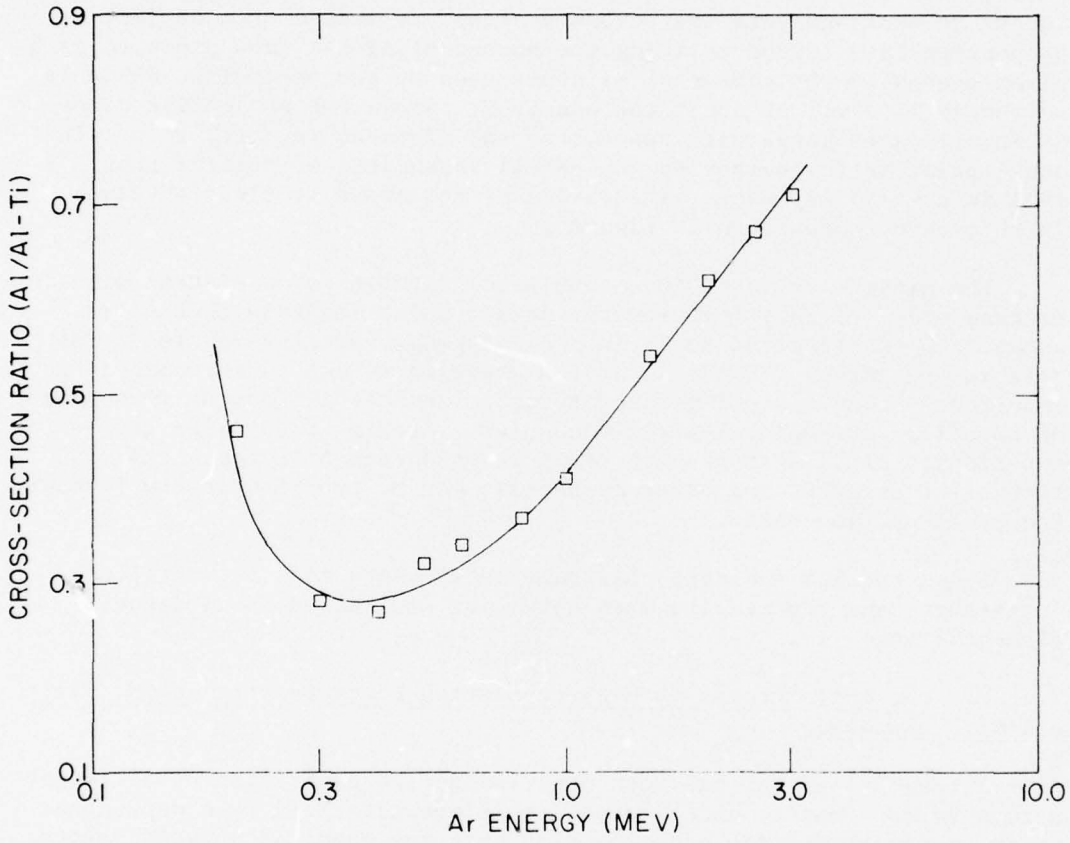


Fig. 3 — The Al K x-ray production cross section measured for an Al target divided by the same cross section measured for a 50 at. % Al, 50 at. % Ti target is presented as a function of the energy of the incident Ar beam

Figure 4 shows high-resolution spectra of Al K x rays excited by 1-MeV Ar ions incident upon (i) pure Al, (ii) 50 at. % Al, 50 at. % Ni, and (iii) 50-50 Al-Ti targets. The leftmost or $K\alpha_{1,2}$ peak results from atoms which have a single K-shell electron removed in the initial state, and the remaining satellite peaks from left to right result from atoms which have respectively *one*, *two*, *three*, . . ., L-shell vacancies in addition to the K-shell vacancy. The spectra in Figure 4 indicate either (a) that 1-MeV Ar ions are relatively less (more) effective in producing multiple L-shell ionization concurrent with K-shell ionization of Al atoms in Al-Ni (Al-Ti) targets than in pure Al, or (b) that those L-shell vacancies, if equally produced in both targets, are more (less) rapidly filled before K x-ray emission in Al-Ni (Al-Ti) than in Al targets.

Chemical effects similar to those shown in Figure 4 were not seen in earlier comparisons of Ne-excited Al Kα spectra from pure Al and Al_2O_3 targets,[1] although chemical effects were seen in the corresponding Kβ spectra. (The Kβ transition in Al involves the valence electrons.) However, Watson, *et al.*[2] have demonstrated differences in the spectra of S Kα x rays produced by 2-MeV/nucleon Ne and O ions incident on Na_2SO_4, S_8, and Na_2S targets. They attribute these observations to explanation (b) because the amount of L-shell ionization observed in the S Kα spectrum is found to be correlated with the valence electron density. They rule out explanation (a) by arguing that there is no reason to expect that the initial S-atom L-shell vacancy distribution produced at the time of the Ne-S or O-S collision will have any significant dependence on chemical environment. In the present experiment, however, it is known[3] that two-step processes (in which Ar 2p vacancies produced in one collision may be transferred to the K-shell of an Al atom in a subsequent collision) contribute to the K x-ray production. Thus explanation (a) cannot be ruled out since Al, Ni, and Ti atoms have widely differing probabilities for producing 2p vacancies in collisions with Ar ions. Indeed, explanation (a) is consistent with the known fact[4] that Ti (Ni) atoms are more (less) effective than Al atoms in producing Ar 2p vacancies in collisions with Ar ions. Thus a higher degree of stripping of Ar projectiles in Al-Ti than in Al might contribute not only to increased Al K-shell ionization but also to a relative increase in L-shell ionization due to electron capture into empty Ar orbitals.

---

[1] P. G. Burkhalter, A. R. Knudson, D. J. Nagel, and K. L. Dunning, Phys. Rev. A6, 6093 (1972).

[2] R. L. Watson, T. Chiao, and F. E. Jenson, Phys. Rev. Lett. 35, 254 (1975).

[3] K. W. Hill and A. R. Knudson, to be published in Appl Phys Lett., 1 May 1976.

[4] F. W. Saris and D. J. Bierman, Phys. Lett. 35A, 199 (1971).

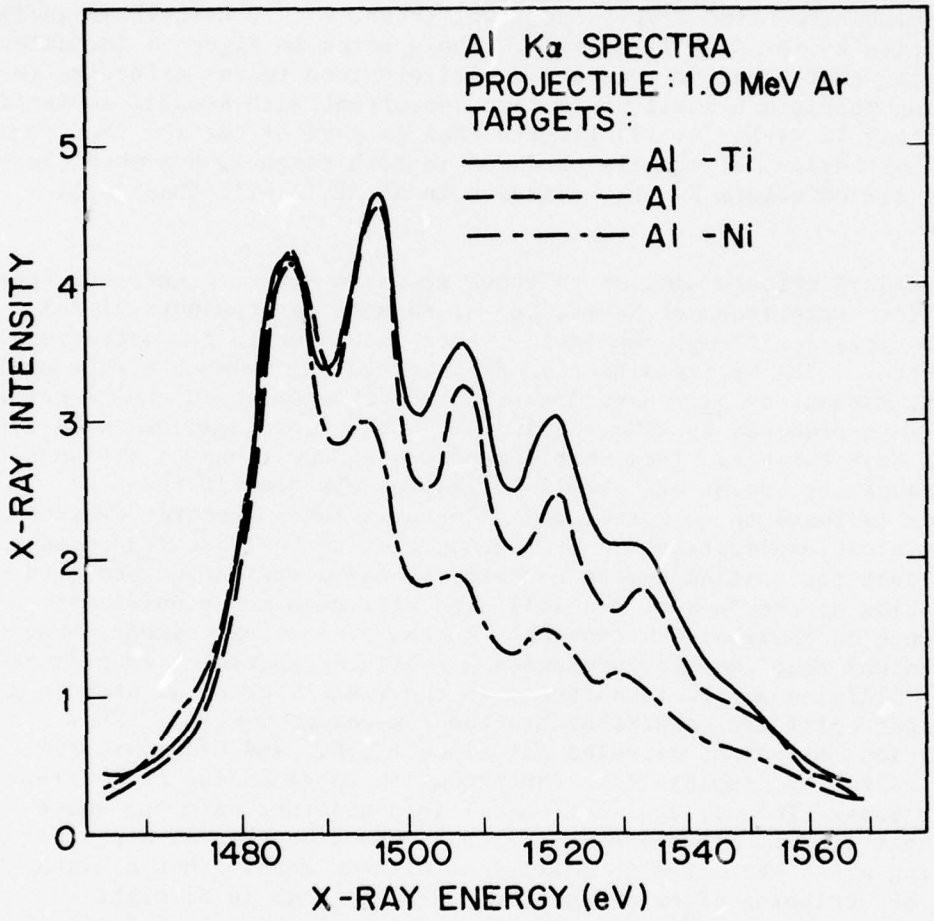


Fig. 4 — Al Kα x-ray spectra from Al-Ti, Al, and Al-Ni targets bombarded by 1.0-MeV Ar^+ ions. The spectra have been normalized at the $K\alpha_{1,2}$ peak at 1487 eV.

Figure 5 indicates that a chemical effect is observed also for Al K x rays produced by 3-MeV He ions incident on Al, Al-Ti, and Al-Ni. However, in the case of He excitation, the intensity of the Kα satellites relative to the diagram line is less in the Al-Ti spectrum than in the pure Al spectrum, in contrast to the result observed for Ar excitation as shown in Figure 4. Since the chemical environment of the Al atom is expected to have no effect on the L-shell vacancy distribution produced by He ion impact, explanation (a) cannot describe the effects seen in Figure 5, and the effect is probably due to explanation (b). This effect, that L-shell vacancies are more rapidly filled for Al-Ti and Al-Ni targets than for pure Al targets, probably also occurs with Ar excitation. Thus this observation implies that the actual difference between the number of L-shell vacancies present in Al and Al-Ti (Al-Ni) targets immediately after excitation by the Ar ion is somewhat greater (less) than the differences in the spectra of Figure 4 indicate.

More data have been obtained for Ar excitation at incident energies of 1.5, 2.0, 3.0, and 7.0 MeV. The data at 3.0 MeV are very similar to the spectra shown in Figure 4. Three-MeV Ne ions produce spectra in which the second satellite is the most intense line in the spectrum, but if the spectra are normalized at the $K\alpha_{1,2}$ peak, the Al-Ti spectrum again lies slightly above the Al spectrum and the Al-Ni spectrum lies below the Al spectrum.

The interpretation of the present data is not clear. Although different electronic vacancy configurations of the Ar projectile are produced in Al, Al-Ti, and Al-Ni targets, probably resulting in different amounts of Al L-shell ionization, it is difficult to determine the extent of the possible influence of recoil effects on the Al Kα spectrum. Recoil effects might produce additional ionization and influence the decay of L-shell vacancies.

F. Ion-excited Vacuum Ultraviolet Spectral Studies (K. W. Hill,* J. Comas,† and D. J. Nagel††)

Ion excited spectral measurements have been useful not only for studying ion-atom collision physics and the structure of ionized systems but also for more applied studies such as materials analysis, determination of sputtering yields, and depth profiling of ion-implanted dopants.

*NRC-NRL Postdoctoral Research Associate
†Electronics Division, Naval Research Laboratory.
††Material Sciences Division, Naval Research Laboratory.

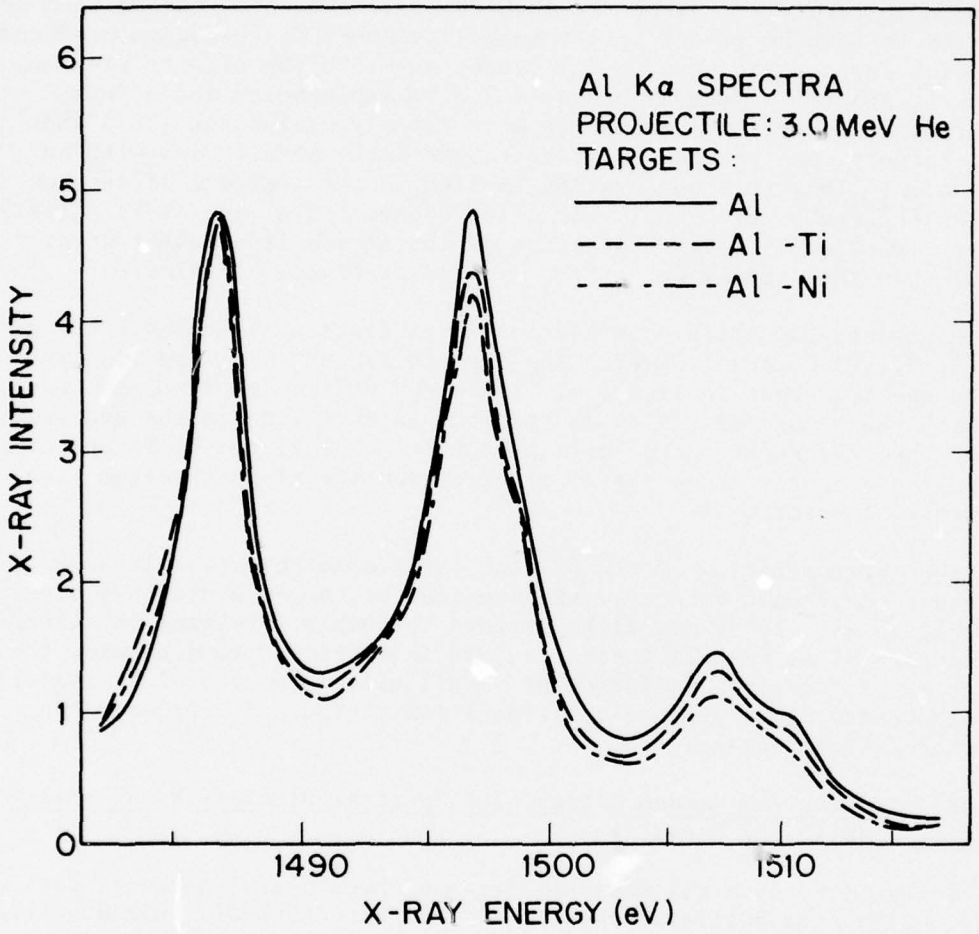


Fig. 5 — Al Kα x-ray spectra from Al, Al-Ti, and Al-Ni targets bombarded by 3.0-MeV He^+ ions. The spectra have been normalized at the $K\alpha_{1,2}$ peak at 1487 eV.

Although ion-excited spectra in the x-ray,[1] XUV,[2] and visible regions have been measured at NRL and elsewhere, very little work has been done with normal-incidence spectrographs in the ultraviolet region. To fill in this gap we have measured spectra excited by ions from the 300-kV ion implantation accelerator in the Electronics Technology Division.

A commercial (McPherson), 1-meter, normal-incidence spectrograph with a 600-line-per-mm grating was set up with its entrance direction perpendicular to the ion beam. Planar targets in a vacuum of 10^{-6} Torr were bombarded at 45° to their normal. Elemental materials (Al, Si, Ti, Ni, Cu, Ag, and Au) and compound semiconductors (SiC, GaP, GaAs, InAs, and InSb) were chosen as targets. Singly-ionized noble gas ions (He, Ne, Ar, and Kr) were used with accelerating voltages of 100 or 200 kV. The spectra were recorded in 800-Å increments, primarily in the 1000-2400 Å region, on Kodak 101-01 film. Examples of spectra centered at 1200 and 2000 Å are exhibited here to illustrate the type of results which were obtained.

Figure 6 is a densitometer trace of the spectrum about 2000 Å which was taken by bombarding Al with a 5-μA beam of 100-keV Ar ions for about 15 minutes. Several spectral lines from singly and doubly-ionized Al (Al II and Al III) are observed. Also present are lines from surface contaminants C and O. Other contaminant species (H and N) are observed at shorter wavelengths. The N and O lines probably result from these gases being adsorbed on the target surface, whereas the C and H lines may result from either ion-induced polymerization of residual hydrocarbons (e.g., from diffusion pump oil vapors) adsorbed on the surface, or from the cracking of such vapors onto the heated target. A weak ArI line was measured at 1048 Å from backscattered excited neutral Ar.

Figure 7 shows the spectrum near 1200 Å obtained from Kr impact on Si at 100 keV. Again, lines from target and contaminant species are evident, with a KrI line appearing at 1236 Å. However, in this region an intense continuum near 1450 Å dominates the spectrum. Continua with similar energies were observed for all projectiles but not all targets. The positions of the continua correlate with the projectile species, as indicated in Figure 8. This contrasts with other work at longer wavelengths, where continua have been observed in ion-excited spectra, but no correlation with projectile species was found.[3]

---

[1] A. R. Knudson, D. J. Nagel, P. G. Burkhalter, and K. L. Dunning, Phys. Rev. Lett. 26, 1149 (1971).

[2] D. J. Nagel, A. R. Knudson, and P. G. Burkhalter, J. Phys. B8, 2779 (1975).

[3] C. W. White, N. H. Tolk, J. Kraus, and W. F. Van der Weg, to be published.

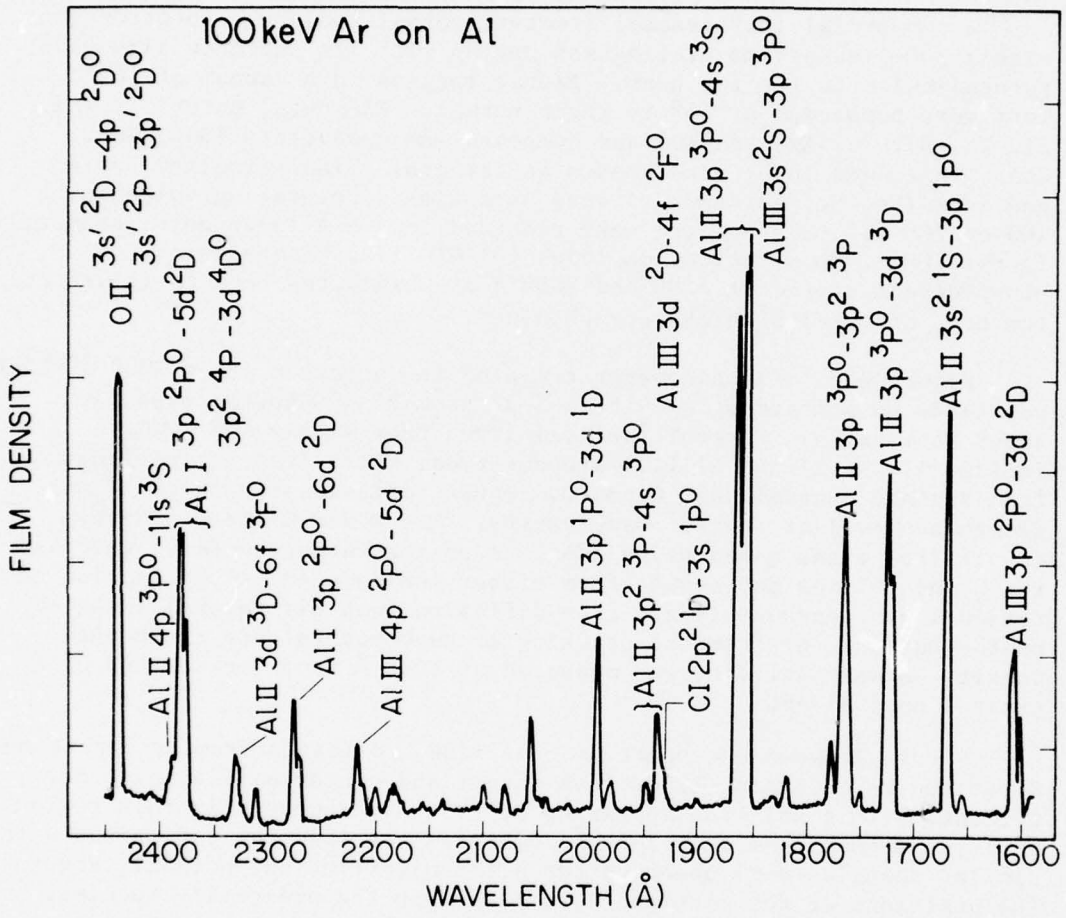


Fig. 6 — Densitometer trace of a spectrum resulting from bombardment of Al with 100-keV Ar ions. Line spectra from target, projectile, and surface contaminant species are present.

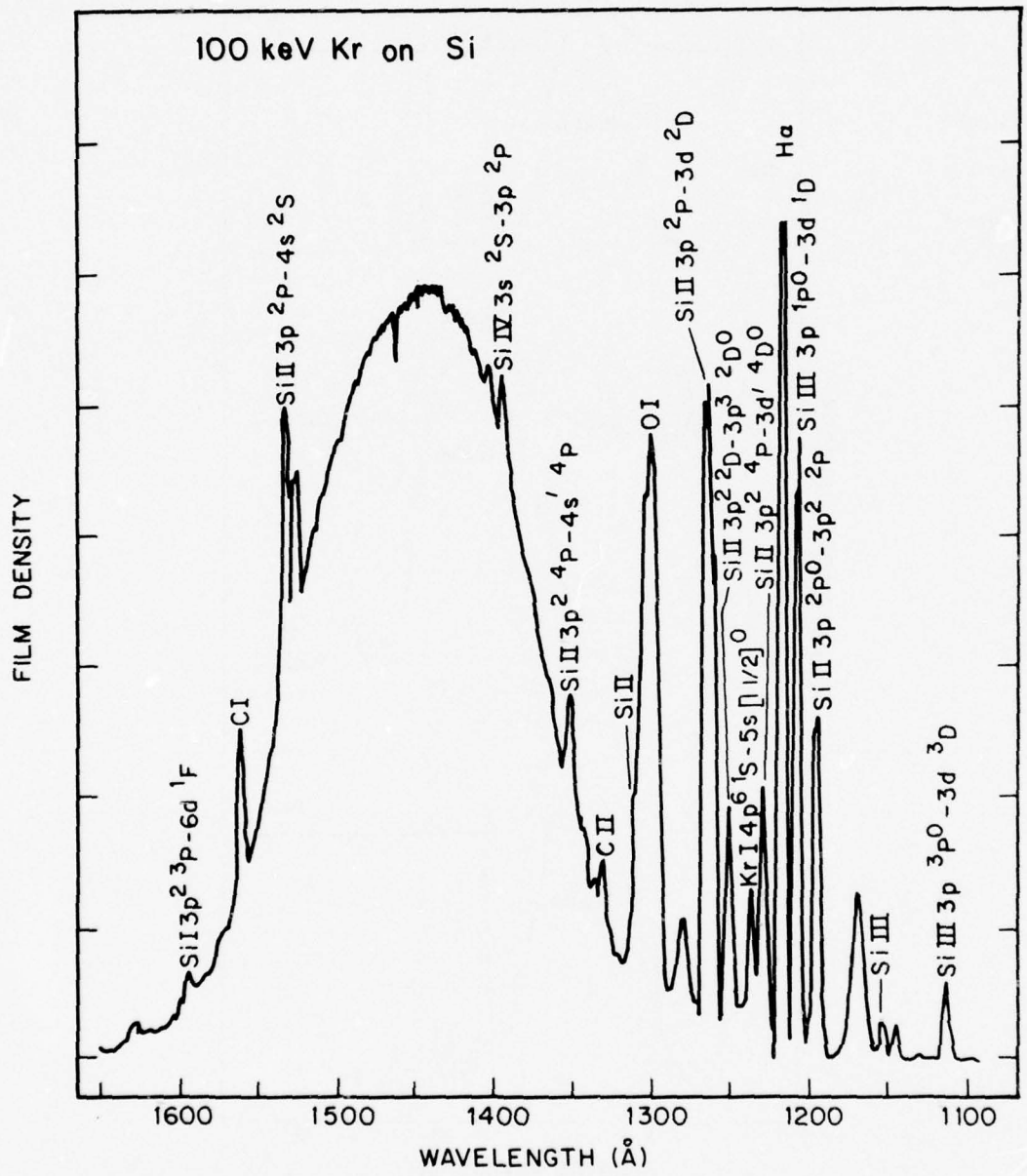


Fig. 7 — Spectrum resulting from 100-keV Kr ion impact on a Si target. In addition to line spectra from target, projectile, and target-surface contaminant species, a strong, broad continuum is observed.

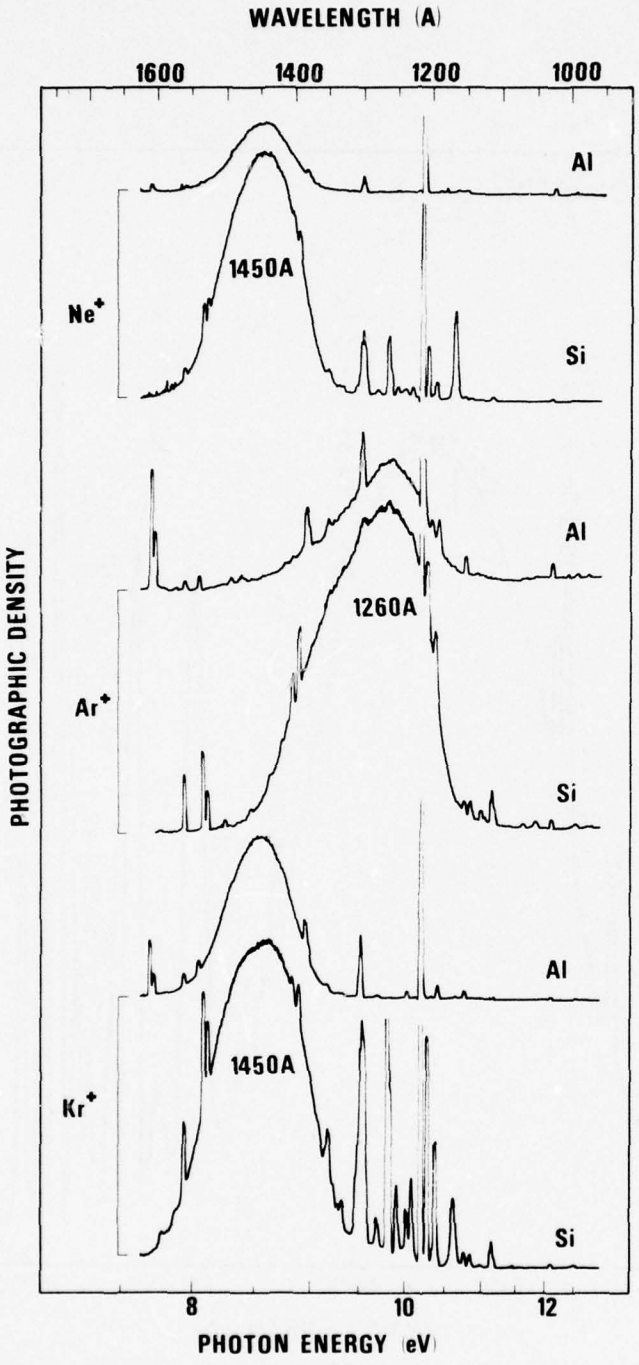


Fig. 8 — Spectra excited by 100-keV Ne^+, Ar^+, Kr^+ incident on Al and Si. The positions of the continuum peaks correlate with the ion beam species rather than the target element.

Interpretation of the spectra in terms of the mechanisms which produce the observed features is in progress. It is clear that the line radiation observed in this work is coming from or in front of the target surface. At higher ion and photon energies, radiation from within a target is observable. However, radiation in the UV region can escape only from the outer layers of a target. Since we observe lines which are sharp (characteristic of free atoms and ions) and not broad bands (typical of solids), it is clear that most of what is observed comes from sputtered and backscattered species near, but not in, the target. Higher ionization stages can and probably are produced by 100-keV ions. However, the ion neutralization process[4] effectively restores electrons to the ions as they leave a surface. Hence, only relatively low ionization stages are observed.

The source of the continua is not clear. Similar spectra are observed below 2000 Å from rare gas ions excited in electrical discharges.[5] They arise from decay of transient excited molecules (excimers) containing two noble gas ions which decay into an unbound state. The continua measured with discharges vary regularly with Z in their position. In contrast to this, we obtain continua which peak at the same wavelength (1260 Å) for He and Ar and at another wavelength (1450 Å) for Ne and Kr. Additional experiments appear necessary to identify the source of the continua. In particular, projectiles other than noble gas ions will be used and the measurements will be repeated at a few MeV with the Van de Graaff accelerator.

In summary, high-resolution measurements of ion-excited UV spectra have been obtained, mainly at 100 keV, for a wide range of projectile-target combinations. Line spectra from neutral or low-ionization stages of sputtered target and contaminant species are observed, along with a few lines from backscattered projectile ions. Newly-discovered continua near 1300 Å remain to be explained.

G. Photographic Image Enhancement by Ion-excited X Rays and Rutherford Backscattering (A. R. Knudson, P. R. Malmberg, and C. D. Bond†)

The Navy occasionally needs to extract information from photographic films that, for one reason or another, have been improperly exposed. Currently available films cease to be of value when underexposure or underdevelopment causes the average optical density* of the image to be

[4]W. F. Van der Weg and P. K. Rol, Nucl. Inst. and Meth. 38, 274 (1965).
[5]Y. Tanaka, A. S. Jursa, and F. J. LeBlanc, J. Opt. Soc. Am. 48, 304 (1958).
†Radiation Technology Division, Naval Research Laboratory.
*Optical density ≡ log (1/transmission)

less than about 0.1. This corresponds to an Ag density of about 2×10^{-5} g/cm^2. At the other extreme, commonly available densitometers cannot measure optical densities greater than about 5. The problem of extracting information from these films is essentially one of materials analysis, namely, measuring the Ag concentration as a function of position on the film.

Trial experiments have been performed with a lantern slide plate Kodak Tri-X film. Rutherford backscattering and ion-excited x rays were used to measure the Ag in both types of film. Proton, He, and Ne beams were utilized for these studies. Even in areas which had not been exposed to light and which appeared to be clear to the eye, the presence of Ag was readily detected by the methods used. The one exception to this situation was the case of Ne-excited Ag x rays. In this case the Ag L x-ray signal from the clear area of the lantern slide was very weak.

The cross section for production of Ag L x rays by protons is given approximately by $\sigma_X = 17.0\ E^{2.1}$ barns/sr, where E is the proton energy. The cross section for Rutherford scattering is given by $\sigma_R = 3.93\ Z_1^2/E^2$ barns/sr at 135°, the angle used in the present measurements. Z_1 is the atomic number of the projectile. For ion energies greater than 1 MeV, the x-ray production cross section is greater than the Rutherford scattering cross section for He. This advantage is somewhat offset by the continuum of x rays emitted as a result of the electrical charging of the film, although this charging problem can probably be reduced or eliminated.

The most significant finding of these experiments was that the depth distribution of the Ag, as indicated by the backscattering measurements, appeared to be different in exposed and unexposed areas of the film. Figure 9 shows the spectra obtained from the backscattering of 2.0-MeV He^+ ions from dark and clear areas of a lantern slide. Figure 10 shows the spectra obtained by scattering 2.5-MeV protons from light and dark areas of Tri-X film. In both cases the Ag distribution seems to be more peaked at the surface in the exposed (dark) areas than in the unexposed areas, where the Ag is due to fog. This result suggests that backscattering may provide a method of discriminating between Ag associated with the image on the film and Ag associated with fog, which provides a background level on which all of the image information is superimposed.

Further experiments are planned with films which have received known exposures and been developed in strict compliance with standard procedures. If the results of these experiments are promising, methods will be developed for obtaining efficiently the Ag concentration as a function of position on the surface of the film. A spatial resolution of the order of 10 micrometers will probably be necessary in order to extract all of the information contained in the film.

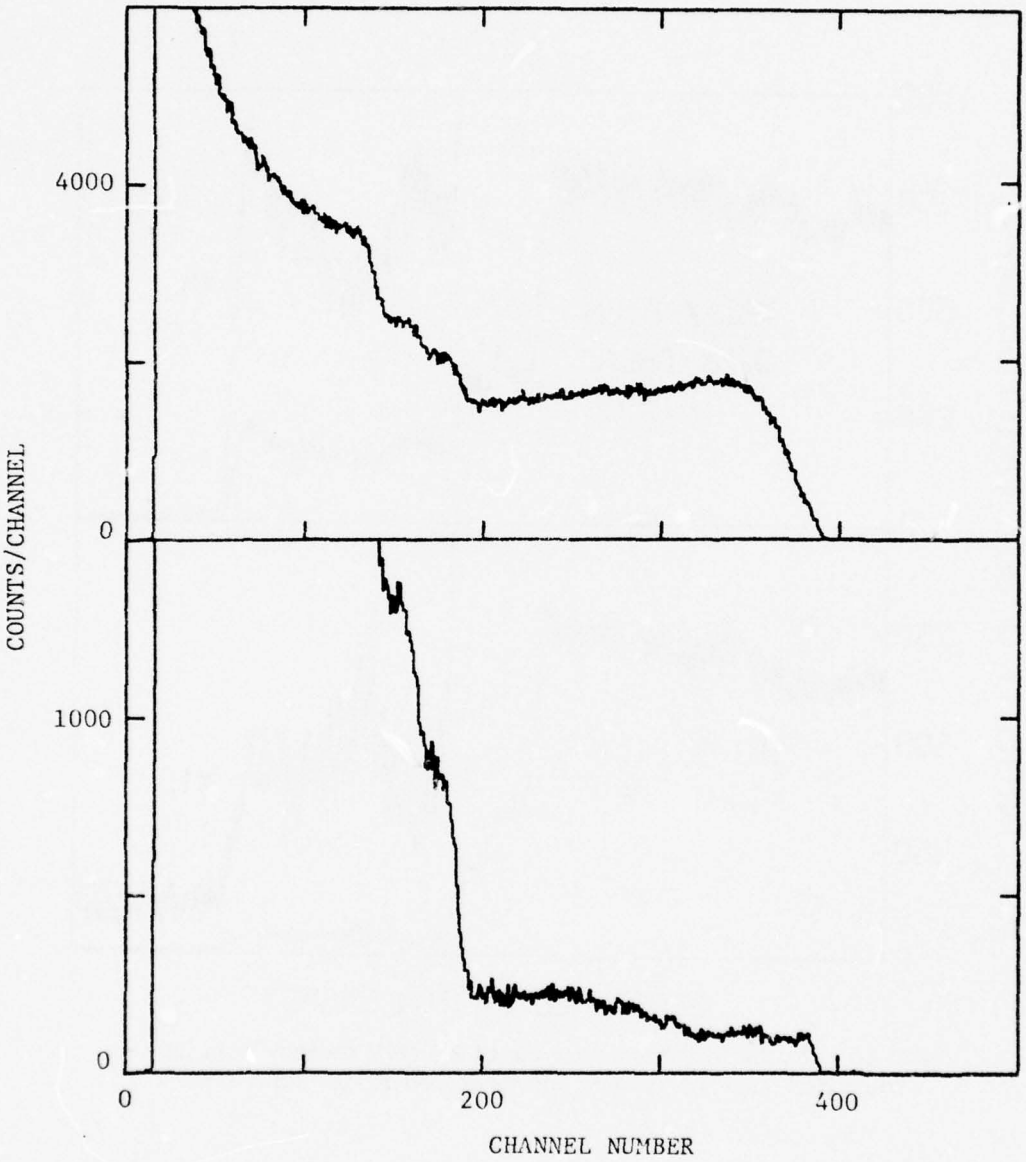


Fig. 9 — Rutherford backscattering of 2-MeV He^+ ions from exposed and developed emulsion on lantern slide plate. At the top is the spectrum obtained from a gray area of the plate and at the bottom the spectrum from a clear area.

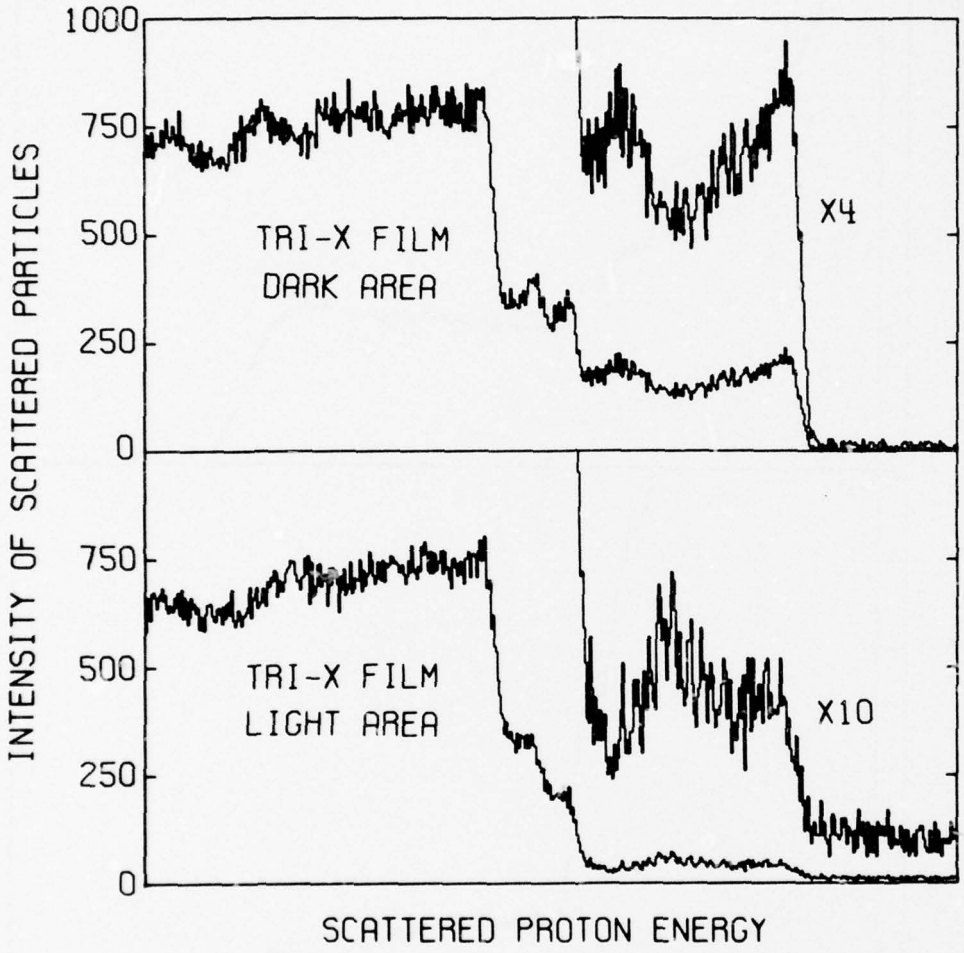


Fig. 10 — Rutherford backscattering of 2.5-MeV protons from light and dark areas of exposed and developed Kodak Tri-X film

H. Measurements of Trace Quantities of Fluorine from Slip-ring Lubricant (J. W. Butler and K. L. Dunning*)

The Surface Chemistry Branch is working on lubrication problems related to slip rings in the inertial guidance system for Polaris missiles. Slip rings in practice have been effectively lubricated with perfluorotributyl amine (FC43) even though it appears to evaporate from the surface in a short time. Conventional efforts have been made to detect and to identify any residual lubricating film; but no evidence of the film was found by ATR infrared spectroscopy, and no high boiling-temperature contaminants were detected by gas chromotography analysis of the distilled lubricant.

The material of the slip rings is simulated by copper coupons (1 cm x 5 cm x 1 mm) with a 50-μm-thick plating of nickel-hardened gold. Two samples were evaluated by resonance nuclear reactions with protons from the Van de Graaff accelerator: sample 1, a coupon on which ten droplets of FC43 were placed and then evaporated to dryness; and sample 2, a coupon which had fourteen similar evaporations. The proton energy was set at 872 keV, which corresponds to a strong sharp resonance in the $^{19}F(p,\alpha\gamma)^{16}O$ reaction. The 5-in. diam NaI(Tl) well-type crystal was used in the anticoincidence mode with an outer plastic phosphor inside the shielded target cave. One of the samples was found to contain about 0.03 μgm F/cm^2 (uncertainty, $\pm$ 50%), and another was found to have about 0.005 μgm F/cm^2 (uncertainty, up or down a factor of two). These uncertainties would have been substantially less if the Van de Graaff vacuum system had not been contaminated with fluorine from three sources: Viton A O-rings, a teflon insulator, and a beam-defining metal diaphragm that had been etched by hydrogen fluoride.

I. Materials Analysis with the Magnetic Spectrometer (J. K. Hirvonen and G. K. Hubler*)

The 20-inch-radius double-focusing magnetic spectrometer (MS) has continued to be utilized for high energy resolution ($\Delta E/E \approx 10^{-3}$) Rutherford backscattering (RBS) measurements. This energy resolution affords much better depth resolution (15 Å - 30 Å) near the surface than is possible with conventional surface-barrier solid-state detectors ($\Delta E/E \approx 10^{-2}$). Scattering measurements on this system have been facilitated by the installation of a multipurpose scattering chamber onto the spectrometer and by the use of a position-sensitive detector (PSD) in the image plane of the spectrometer. This system is described in detail in the previous NRL Van de Graaff operations report.[1]

*Radiation Technology Division, Naval Research Laboratory
[1]NRL Memorandum Report 3078, July 1975.

This spectrometer has been used in nuclear backscattering, nuclear reaction, and particle channeling experiments. Some experimental results are presented here to demonstrate the advantages a magnetic spectrometer may have over a conventional solid-state detector for certain types of experiments; viz., (i) superior mass resolution, (ii) superior (X10) depth resolution, and (iii) superior sensitivity (>10X) for impurity detection or for depth distribution profiling. In practice, the extent to which a spectrometer's superior energy resolution can be exploited for surface analysis may be limited or complicated by several factors, such as energy-loss straggling, kinematic broadening, isotope effects, surface roughness, surface oxides and other contaminants, aberrations of spectrometer optics, and ion-beam-induced target damage. Some of these factors are discussed, and the extent to which they limit or complicate the sensitivity of high-resolution spectrometers for surface analyses is illustrated by experimental data. The particular experiments from which data are taken are not discussed in detail here. These experiments merely illustrate different aspects of using high-resolution magnetic spectrometers as a technique in materials analysis.

Mass and Depth Resolution

Figure 11 illustrates several features of high-resolution backscattering. An obvious difference between the solid-state detector and magnetic-spectrometer spectra for channeling along the ⟨110⟩ direction of GaAs is the resolving of the ^{69}Ga, ^{71}Ga isotopes in the latter. This better mass (depth) resolution allows a higher sensitivity to the near-surface region for channeling investigations (e.g., minimum yield measurements, surface peak structure, near-surface damage). In return for this improvement, the increased energy dispersion requires a corresponding increase in analyzing beam charge for comparable statistics. In addition, the analyzing beam spot must be kept relatively small (<1 mm^2) in order that the resolution will not suffer as a result of the (magnetic) optics of the spectrometer. Hence, to ensure that the analyzing beam does not produce significant target damage, movement of the target or the beam spot may be necessary.

It is also seen that the width of the various surface peaks are appreciably wider than the system resolution for the case of the spectrometer spectrum. This is mostly attributed to the thickness of the native oxide on the GaAs. However, kinematic broadening can make a significant contribution to the relative widths of peaks or edges measured by high-resolution backscattering. For example, a spectrometer input solid angle of 2.5 msr used here contributes a kinematic energy spread of nearly 3 keV to the Ga or As surface peaks for incident 2-MeV He ions. The kinematic energy spread increases for lighter target atoms and for larger input solid angles and would be, for example, about 5 keV for 2-MeV He scattering from silicon for the same solid angle (2.5 msr). This contribution alone is significantly larger than the system resolution and often forces a compromise between resolution achieved and practical counting rates.

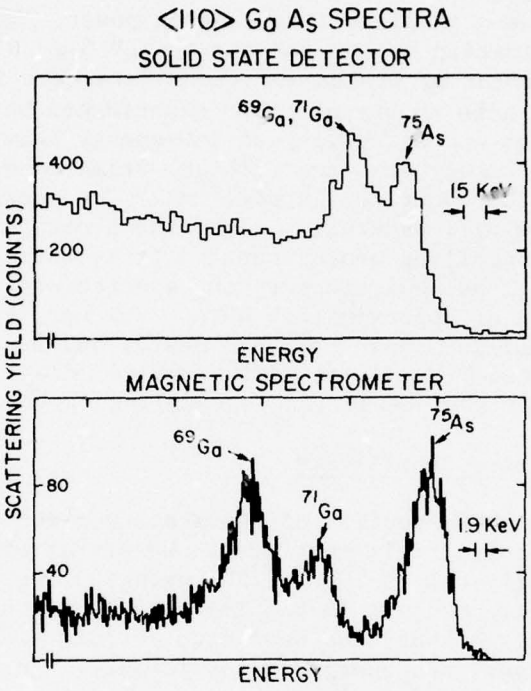


Fig. 11 — Solid-state detector and magnetic spectrometer backscattering spectra for He ions incident along the ⟨100⟩ direction of GaAs

Another example of the depth resolving capabilities of magnetic spectrometers is shown in Figure 12. This figure shows a series of spectra taken of 2-keV to 60-keV energy ^{209}Bi implantations into pre-implanted (5×10^{14} Ar/cm^2 at 60 keV) silicon. The depth scale was calculated assuming constant but different stopping powers for the incident 2-MeV He^+ ion beam and the scattered He^{++} ion beam, and ignoring the contribution of the implanted ^{209}Bi to the stopping power. This should be a reasonable approximation except for the 40-keV 5×10^{16} Bi/cm^2 implantation. The point of presenting these data here is not to make a detailed comparison with theory or other experiments but to illustrate that projected ranges and straggling of low-energy heavy ions in light substrates can be directly measured with an estimated depth resolution less than 30 Å near the surface (in silicon). The energy-loss straggling of the analysis beam will eventually limit the depth resolution attainable in such depth profiling measurements. It is estimated that the straggling width will be equivalent to the spectrometer resolution for scattering depth of approximately 40 Å. However, the measured widths of the Bi profiles shown here are mostly due to the range straggling of the implanted Bi ions and would only decrease by 5% to 10% if account were taken of the energy-loss straggling of the analyzing beam.

Impurity Detection Sensitivity

The fact that only a portion of the scattered-ion spectrum is analyzed at one magnetic field setting can be either disadvantageous or beneficial. Typically only a 10% to 15% energy slice of the scattered particles can be well resolved in the image plane of the spectrometer. If a single conventional position-sensitive detector is used to detect the particles, the analyzed energy region (about 2% in our system) will be further reduced. If one is interested in studying only the surface or an interface, this limitation may present no problems; but analysis over an extended energy region necessitates collecting a number of scattering spectra with a different magnetic-field setting for each. However, the fact that only a small energy slice is analyzed at one time allows a means of avoiding pulse pile-up or interference from other particle groups. Although pulse pile-up can be considerably reduced by electronic means or can sometimes be circumvented by the use of heavy incident analyzing ions (e.g., $^{12}C^+$), the application of a magnetic spectrometer can yield significantly better detection sensitivities for heavy impurity atoms on light substrates without (i) the loss of energy resolution or (ii) the necessity of using heavy analysis beams.

Figure 13 shows the depth distribution of implanted ^{69}Ga atoms (3.5×10^{14} Ga/cm^2 at 60 keV) in silicon both before and after an annealing treatment in an effort to look for redistribution of the implanted ^{69}Ga.[2] It was not feasible to do this by means of a solid-

[2]Unpublished work in collaboration with H. B. Dietrich, Electronics Technology Division.

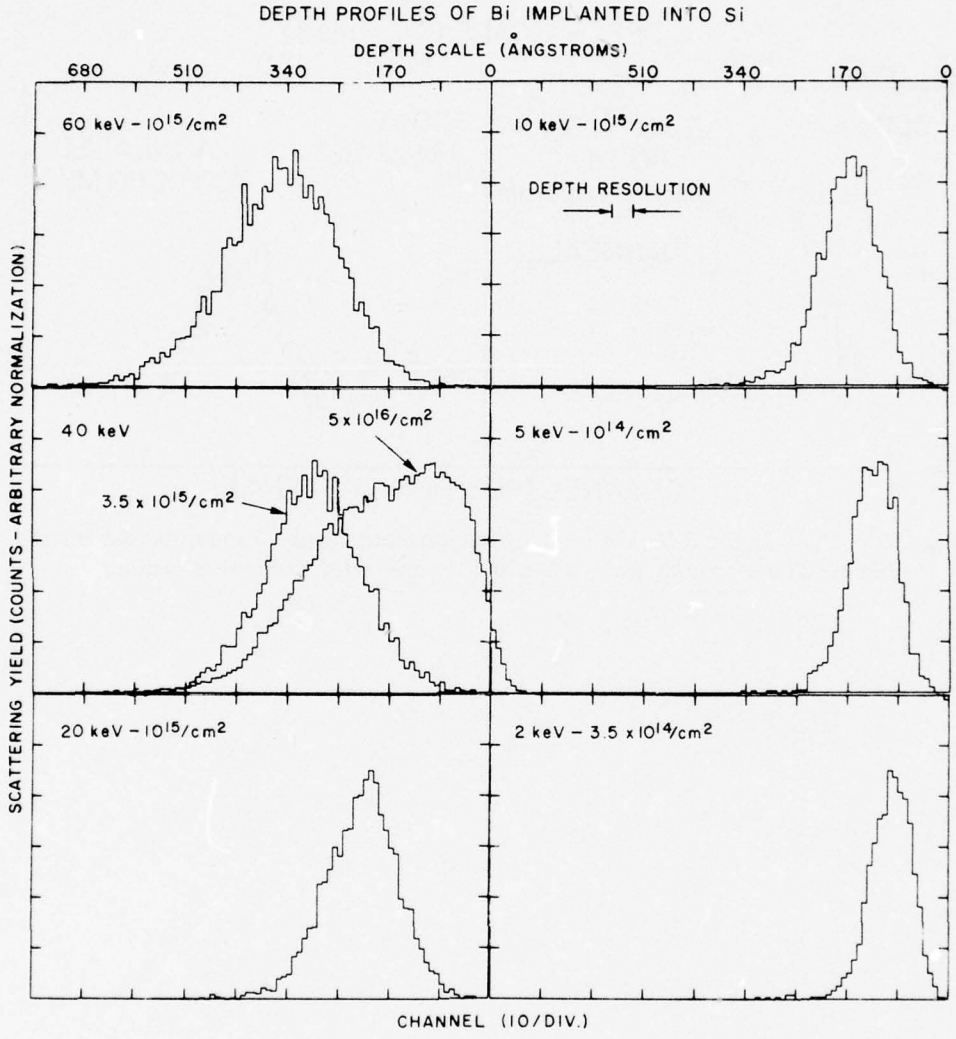


Fig. 12 — Spectra for 2-MeV He ions backscattered from ^{209}Bi atoms implanted into silicon at energies from 2 keV to 60 keV. The depth scale shown at the top is approximate.

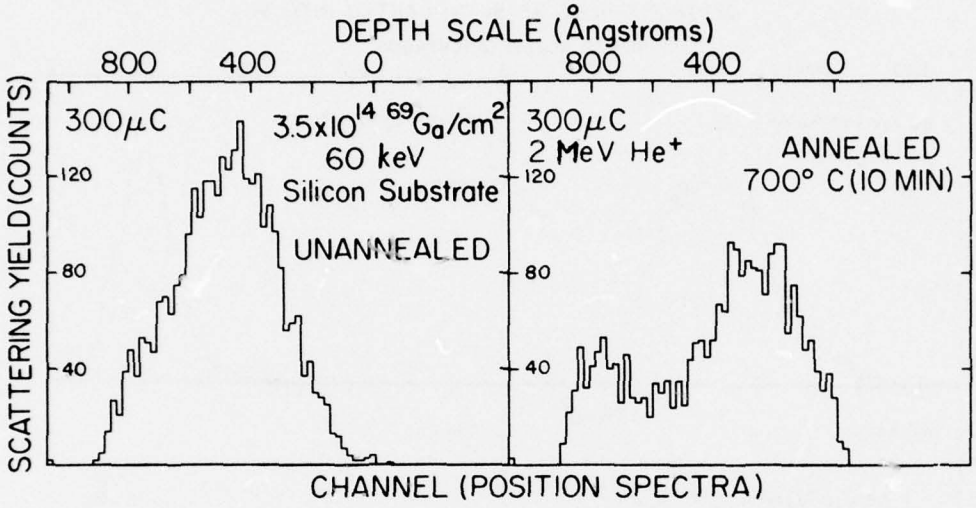


Fig. 13 — Spectra for 3-MeV He ions backscattered from ^{69}Ga implanted into silicon. These spectra were taken before and after thermal annealing.

state detector mainly because of pile-up problems and also because of inadequate depth resolution. However, it was relatively straightforward with the spectrometer in spite of the relatively large amount of analyzing beam charge accumulated (distributed over several adjacent target areas).

These examples illustrate that applying a magnetic spectrometer to near-surface analysis offers substantially better energy resolution than that obtained by use of solid-state detectors. This improved energy resolution provides a correspondingly better depth and mass resolution. It also offers means of avoiding pulse pile-up or interference from other particle groups. In practice, the extent to which a spectrometer's superior energy resolution can be exploited for surface analysis may be limited or complicated by several factors (e.g., energy-loss straggling, kinematic broadening) which must be avoided or accounted for in order to exploit fully the potential advantages of such instruments.

J. Techniques for Deep Profiling of Aluminum in Silicon-on-Aluminum-Oxide Structures by Means of the $^{27}Al(p,\alpha)^{24}Mg$ Reaction (K. L. Dunning*)

A need has arisen in connection with silicon-on-sapphire semiconductor device technology for accurate depth concentration profiles of aluminum to depths up to one micrometer.

The method developed and used for profiling aluminum in silicon, silicon dioxide, and silicon carbide [based upon a sharp resonance at 991.90 keV in the $^{27}Al(p,\gamma)^{28}Si$ reaction] is very useful for profiles in cases where the aluminum is confined to depths of a few thousand angstroms but is much less suitable for structures with deep aluminum-oxide substrates because of the excitation of resonances at energies below 991.90 keV by energetic protons in the substrate.

This method gives best results when a constant fraction of the reactions associated with a single resonance is counted for a pertinent set of bombarding energies. The difficulties associated with the detection of events from more than one resonance would be eliminated or greatly mitigated if a detector of energy resolution much better than 10% were used. (The well-type sodium-iodide detector, which is presently used because of its high efficiency for gamma-rays, has a resolution of about 10%.)

A technique has been developed for profiling aluminum in $Si\text{-}Al_2O_3$ structures to depths of at least one micrometer by means of a resonance at 1364.8 keV in the $^{27}Al(p,\alpha)^{24}Mg$ reaction. The resonance has a published full-width-at-half-maximum value of 1.4 keV. The method will be useful for profiling aluminum in other materials also.

*Radiation Technology Division, Naval Research Laboratory.

The alpha particles are detected by means of a position-sensitive semiconductor detector in the image plane of the reaction-particle magnetic spectrometer described in the preceding section.

Because energy straggling causes spreading of the alpha-particle energy distribution and because the position-sensitive detector spans only about 2.3% of the central alpha-particle energy, not all of the alpha particles can be detected with one setting of the spectrometer magnetic field. Therefore to obtain a constant fraction of the resonance alpha particles emitted at each bombarding energy, it is necessary to reset the spectrometer magnetic field several times for each bombarding energy. The deeper the region being probed, the greater the number of resets required because of the increase in straggling of the alpha particles with depth. This effect can be minimized by choosing a target-beam geometry in which the alpha path is minimized. The effective length of the position-sensitive detector is about 4.5 cm. An improvement could be made by spanning the entire image plane of the spectrometer with a detector several times the length of the present one.

K. Software for Nuclear Resonance Depth-concentration Profiles (P. R. Malmberg and K. L. Dunning*)

Sharp resonances in nuclear reactions (gamma-ray or charged-particle emission) enable a beam of protons to be used as a sensitive probe for measuring the concentration of impurity atoms as a function of depth near the surface of a solid material. In effect, one compares the experimental yield curve (e.g., gamma-ray counts vs. the bombarding energy) with calculated yield curves based on various assumed depth concentration profiles. Precise determination of the profiles requires accurate calculations of the resultant yields. The complexity of these calculations prescribes the use of a high-speed digital computer.

The original software to do these calculations was written for the NRL CDC-3800 computers for use in a batch processing mode. A suitable profile is found by an iterative process with successive trial concentration functions (each choice based upon the result of the preceding trial) until satisfactory agreement with the experimental data is obtained.

Because of a turnaround time and the necessity for preparing profile data cards, the overall procedure is slow. Consequently, efforts have been started to develop software for the SEL 840A computer (dedicated to the 5-MV Van de Graaff) to do the actual fitting process in a mode involving prompt interaction with the operator. This process will utilize large transformation matrices calculated by a large computer.

*Radiation Technology Division, Naval Research Laboratory.

The program (YMAT) to calculate the large matrices was obtained by a major modification of the original profile fitting program. This program has been written and debugged; and correct operation has been verified not only by a special test program for the CDC-3800 computer, but also by checking that the matrix could be transferred (via magnetic tape) to the SEL 840A computer and used to give identical calculated yield results.

The program (MXPR) to perform the fitting of data using the SEL 840A is sufficiently large so that individual portions of it have to be used by disc swap. Elements of the program involve input/output, plotting, calculations, and oscilloscope use. The heart of the program is the use of the oscilloscope--with which calculated yields can be promptly seen and compared with experimental data, and the successive trial concentration functions can be generated by means of a light pen. Because the matrices calculated by the larger computer are too big for storage in core memory of the SEL 840A, they are stored on the disc and transferred a row at a time for use. Because of these transfers, the necessary matrix multiplication operation is slow; nevertheless the process takes only 45 seconds for a 5400-element matrix. Writing of the program was finished in 1975. The major debugging of all portions except the oscilloscope section is completed. Debugging of the oscilloscope portion, which is the most difficult part, is continuing.

L. The Treatment of Energy-loss Fluctuations in Surface-layer Analysis by Ion Beams (J. W. Butler)

When surface layers are probed by charged particles, the particle energy scale is ordinarily used to obtain the depth scale. However, the energy-loss process is statistical in nature, resulting in fluctuations in energy losses and a corresponding degradation of depth resolution. Therefore, one needs an accurate theory of energy-loss processes to transform from an energy to a depth scale. But for protons used in nuclear-reaction analyses or Rutherford backscattering analyses on targets with atomic number (Z) higher than about 14 (silicon), existing methods of treating the problem of fluctuations in energy losses among the different particles in an analyzing beam are inadequate. For example, conventional theoretical distributions tend to be too broad. Present methods of calculating distributions are valid for medium- and high-Z materials only at high energies ($>10^2$ MeV). The present work (a) proposes a modification of current theory so that the energy-loss distributions for low-energy protons on medium- and high-Z targets can be predicted with reasonable accuracy, (b) describes experimental measurements of the distributions of energy losses for 1-MeV protons on a low-Z target (nitrogen) and a medium-high-Z target (xenon), and (c) compares theory with experiment.

Bethe's equation[1] for the average energy loss ΔE_a of a heavy charged particle with speed $v = \beta c$ and charge ze in a thin layer of matter may be written in the following *unconventional form:*

$$\Delta E_a = 2\xi\left(\ln \frac{E_m'}{I} - \beta^2\right), \qquad (1)$$

where ξ is proportional to target thickness and to the target atomic number Z and is in energy units, where $\underline{I}$ is the average ionization potential of the target material, and where E_m' is the maximum energy that can be transferred to a stationary free electron in a collision with the incident particle.

Bethe's equation was derived under the assumption that the incident particle speed v is much greater than the Bohr-orbit speed v_K of the K-shell electrons in the target material. However, much of the application of ion beams to surface-layer analysis involves cases in which the target K-shell electrons have speeds comparable to or greater than the incident particle speed. For example, the K electrons in silicon have a Bohr-orbit speed about equal to that of a 3-MeV proton; and the K electrons in tantalum have a speed about equal to that of a 120-MeV proton. Furthermore, it is obvious that Eq. (1) is not applicable to situations in which $I \geq E_m'$ because in such cases the logarithm term is either zero or negative. The assumptions under which Eq. (1) was derived require that $E_m' >> I$.

For situations in which Eq. (1) is applicable, the distributions of energy losses for incident particles have been calculated by Landau[2] for very thin targets and by Symon[3] and Vavilov[4] for moderately thin targets. However, no satisfactory theory exists for cases in which Eq. (1) is not applicable (i.e., for cases in which the incident-particle velocity is comparable to or less than v_K).

The conventional value of $\underline{I}$ is the logarithmic average of ionization potentials (or binding energies) of all the electrons in the atom with a suitable weighting factor. For high-energy incident protons ($E > 10^2$ MeV) such a value of $\underline{I}$ is a reasonable approximation to the actual average minimum energy transferred during a proton-electron collision. But for low-energy protons and high-Z target atoms the more tightly bound electrons have binding energies that greatly exceed E_m'. Hence these electrons do not effectively participate in the energy-loss process. Therefore it appears improper in such cases to use the same value of $\underline{I}$ as is used for high-energy incident protons.

---

[1] H. A. Bethe, Z. Physik, 76, 293 (1932).
[2] L. Landau, J. Phys. (USSR), 8, 201 (1944).
[3] K. R. Symon, "Fluctuations in Energy Lost by High Energy Charged Particles in Passing Through Matter," Ph.D. Thesis, Harvard University (1948).
[4] L. Vavilov, Zh. Eksp. Teor. Fiz., 32, 320 (1957); English translation in JETP, 5, 749 (1957).

The present proposal then is to consider in calculating $\underline{I}$ only those electrons that actually participate under the circumstances at hand.

Toward this end a detailed set of calculations has been made to ascertain which electrons participate in the energy loss process and which do not for proton energy from 0.1 to 100 MeV and for target Z from 6 to 82. Then the "effective" value of Z was defined to be the number of participating electrons, and the effective value of $\underline{I}$ was defined to be the average ionization potential of the participating electrons.

A number of energy-loss distributions have been measured for 1-MeV protons passing through various selected materials from Z = 7 (nitrogen) to Z = 54 (xenon).

The experimental procedure involved passing a 1-MeV beam of protons from the Van de Graaff accelerator through (i) the 2-meter electrostatic analyzer set to give a beam-energy resolution of 0.02% and (ii) then through a differentially pumped gas cell (effective length: 20 cm) containing the desired material for slowing the protons. The energy distribution of the transmitted beam was then measured by a narrow p,γ resonance as an energy filter. The resonance chosen is the 992-keV resonance in the $^{27}Al(p,\gamma)^{28}Si$ reaction. The target was an evaporated layer of aluminum on a smooth layer of copper which in turn was deposited onto a disk made from microscope-slide glass. The average energy loss of the beam in the target was about 150 eV. The full width at half maximum of the experimental resonance curve was less than 300 eV when no gas was in the cell. Since the energy filter on the transmitted beam was fixed in value, the distribution of output energies was measured, in effect, by a sweep of the input energy through the desired range.

For 1-MeV protons penetrating a nitrogen target, conventional theory should give good results because E_m' is substantially larger than the binding energy of the K-shell electrons. And the application of conventional theory gave good agreement with the experimental measurements.

However, for 1-MeV protons on xenon, it is reasonable to expect conventional theory to fail because E_m' is about 2 keV whereas the xenon K electrons are bound by 35 keV, and L electrons are bound by about 5 keV. And indeed we observe that conventional theory does fail in this case. The broken curve in Figure 14 shows the experimental reaction yield curve (in essence, the energy-loss distribution curve) for a xenon pressure that produced an average energy loss of 2680 eV. The solid curve labeled "I = 555 eV" shows the distribution predicted by conventional theory. Note that this distribution is so broad that it even predicts some energy gains. The curve labeled "I = 148 eV" shows the theoretical distribution predicted with the "effective" values of Z and $\underline{I}$ as proposed herein. The agreement is within experimental uncertainty.

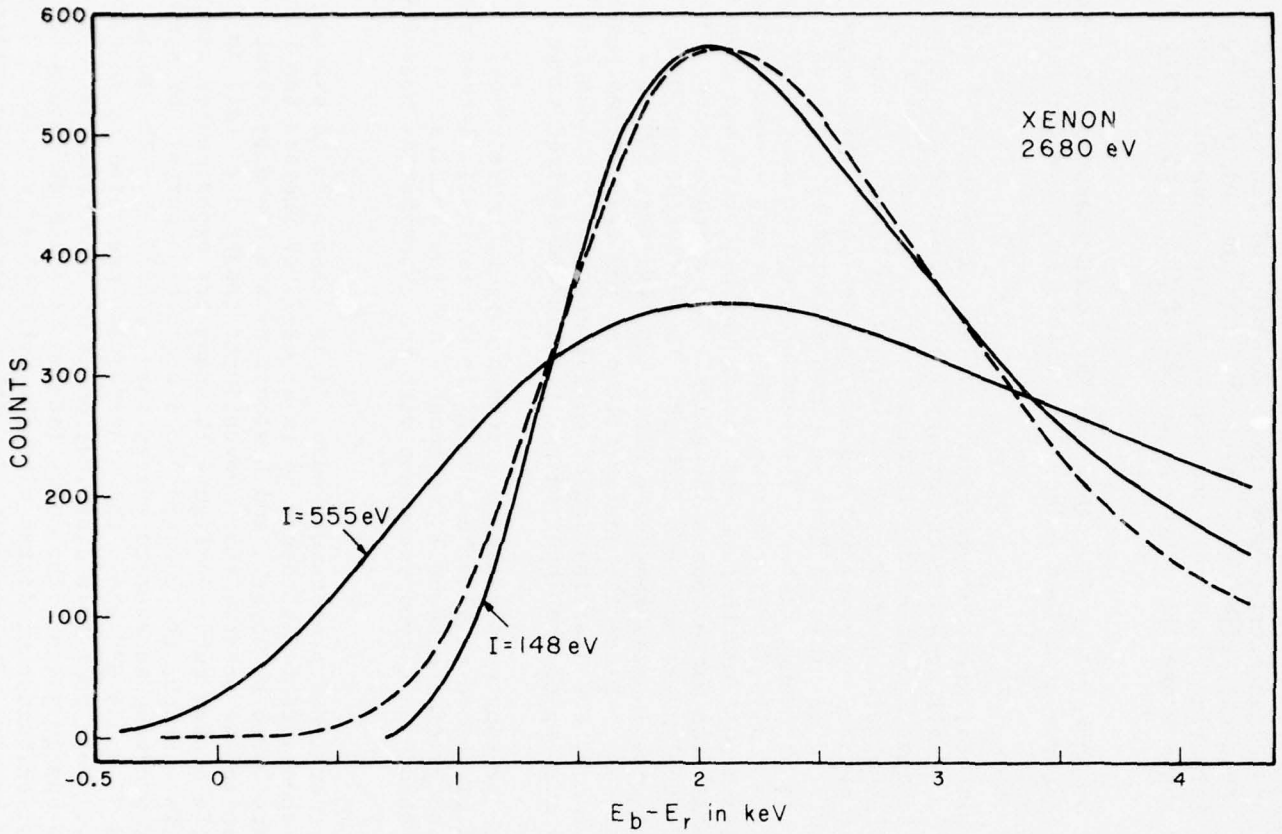


Fig. 14 — Resonance yield curve (essentially the energy-loss distribution curve) for protons passing through the gas cell containing enough xenon to provide an average energy loss of 2680 eV. The broken curve is the experimental distribution. The solid curve labeled "I = 555 eV" shows the energy-loss distribution predicted by conventional theory. The solid curve labeled "I = 148 eV" shows the energy-loss distribution predicted by the theory as modified herein.

Future plans include the application of the concept of effective values of Z and I to specific problems of surface-layer materials analysis with ion beams.

M. Reduction of Wear of Sliding Surfaces by Ion Implantation (J. W. Butler and J. K. Hirvonen)

In October 1975, a research program was begun to improve the wear resistance of surfaces by means of ion implantation.

Part of an AISI-52100 steel ball (of the type widely used in ball bearings) and part of an AISI-52100 steel race (from a roller bearing) were implanted with about 10^{17} nitrogen ions per cm^2 at an incident energy of 40 keV. Then the ball was held stationary against the race, which was rotated by a lathe as illustrated in Figure 15. A dead-weight load pressed the ball against the race, which dipped into a pool of synthetic polyester jet engine oil (Mobil Jet Oil II, meeting MIL-L-23699 specifications). The contact pressures varied in different runs from roughly 100 bar to roughly 10000 bar. The wear was measured by optical-microscope examination of the wear scar on the ball. The Archard wear parameter K (which is a dimensionless measure of the wear volume with the effects of load, hardness, and distance normalized out) was then calculated and plotted as a function of distance traveled. The upper curve in Figure 16 shows the value of K when an unimplanted spot on the ball slides on an unimplanted track on the race. Here the load was 3.6 kg, which provided contact pressures from about 10 kbar to about 1 kbar, depending on the contact areas at different times during a run. The lower curve in Figure 16 shows the value of K for an implanted spot on the ball sliding on an implanted track on the race. The improvement in wear by the implantation was roughly a factor of two. The result is rather surprising because the depth of the wear scar on the ball at the maximum running distance represented by Figure 16 is roughly 1000 times the depth of the implanted nitrogen ions; yet the improvement in wear resistance appears to increase with distance traveled.

Figure 17 shows a set of curves obtained with a lower load (by about a factor of ten) than that used for Figure 16. The improvement in wear resistance is again about a factor of two. But Figure 17 also includes a run wherein an unimplanted spot on the ball was sliding on an implanted track on the race. Here, except for the first "break in" point, the improvement in wear resistance was approximately the same as in the implanted-on-implanted case.

Several experiments have been made to test various hypotheses about the mechanism for the wear improvement. For example, the Van de Graaff accelerator was used in an attempt to detect nitrogen [by means of the $^{14}N(d,p)^{15}N$ reaction] under the wear scar on the ball. The hypothesis here was that the implanted nitrogen possibly migrated under local high temperatures and pressures, with a significant amount always remaining under the scar. In the nuclear-reaction test, a small amount

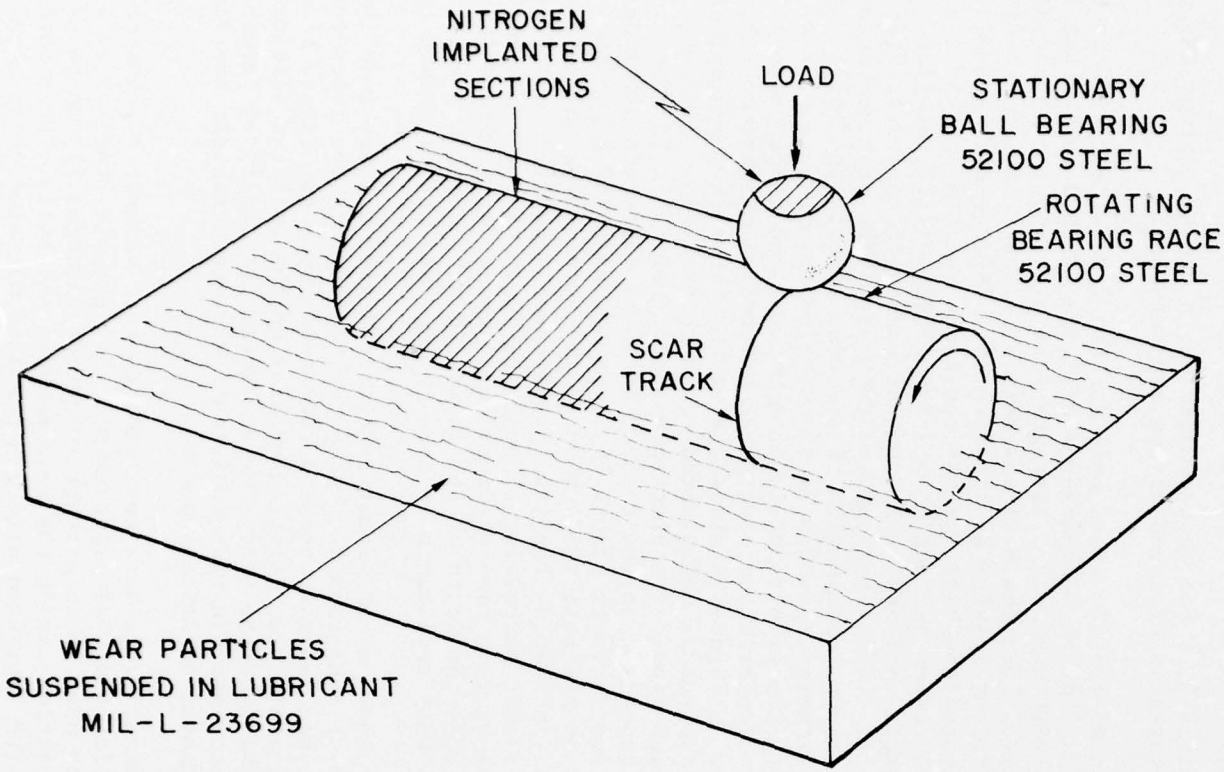


Fig. 15 — Experimental arrangement for testing the relative wear resistance of AISI-52100 steel-bearing surfaces (unimplanted and nitrogen-implanted)

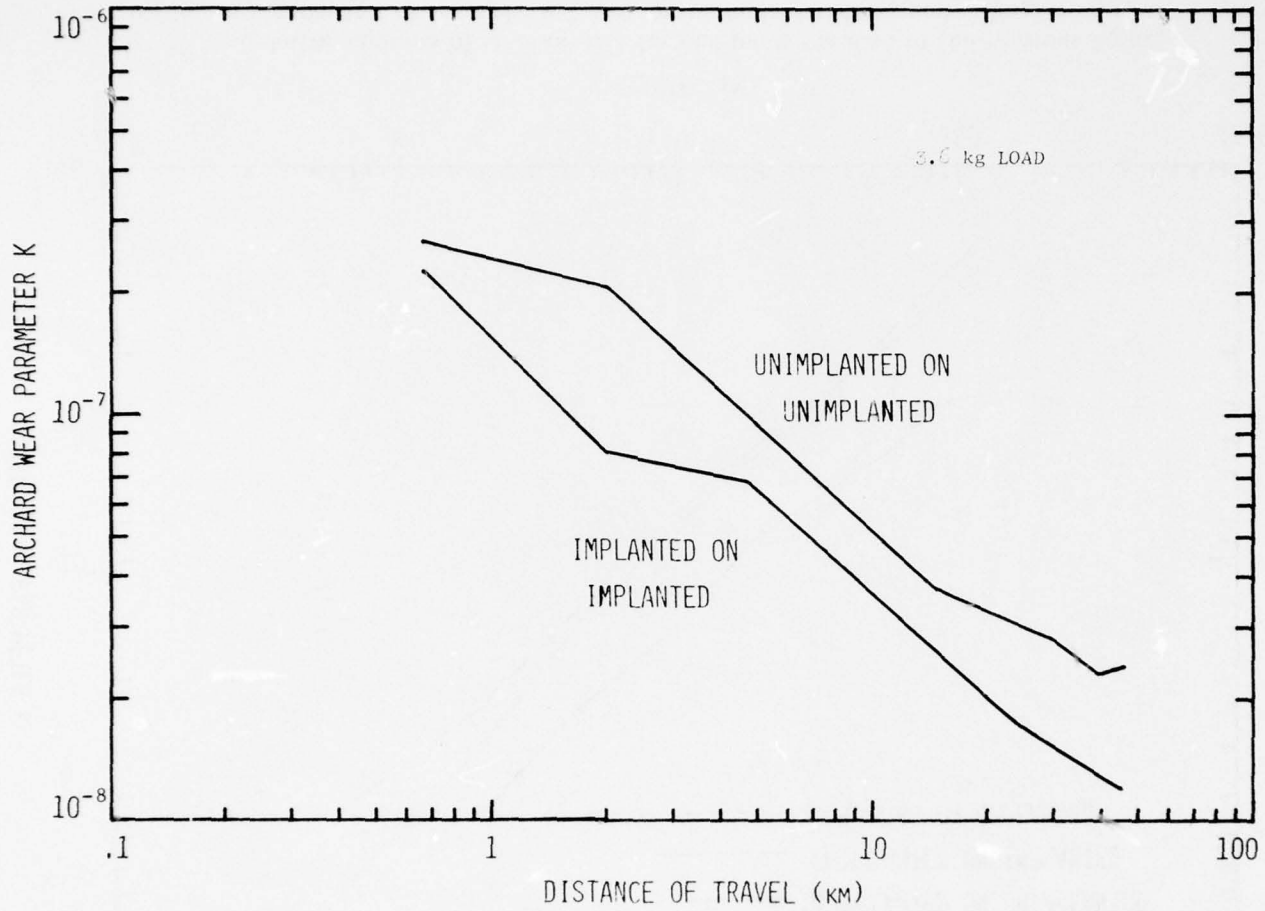


Fig. 16 — Relative amounts of wear on the ball when an unimplanted spot on the ball rubs an unimplanted track on the race (upper curve) and when an implanted spot rubs an implanted track (lower curve)

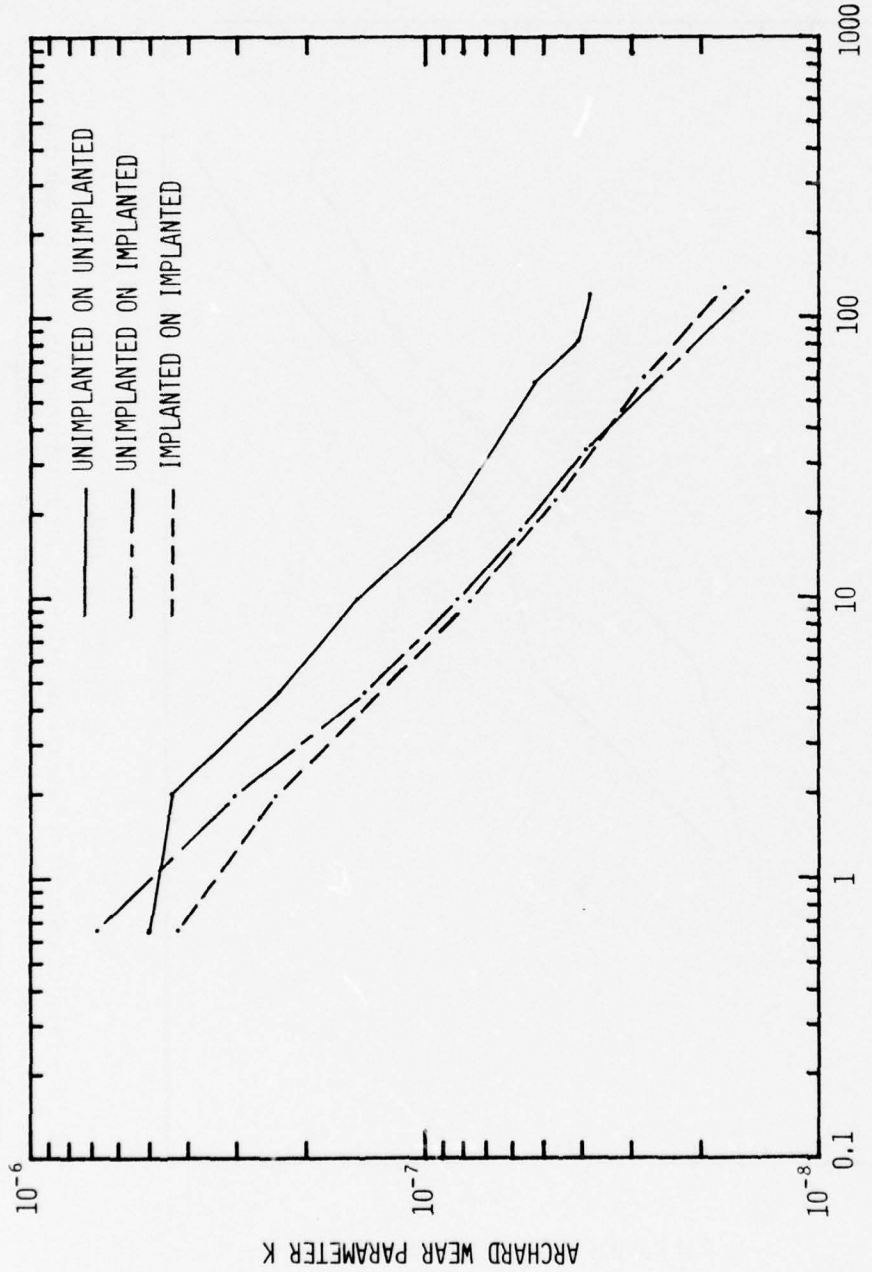


Fig. 17 — Relative amounts of wear on ball for one-tenth the load of the previous figure, including a comparison of unimplanted spot on unimplanted track and unimplanted spot on implanted track

of nitrogen was detected just under the scar, but a roughly equal amount was detected also on the unimplanted section of the ball. Hence this test was inconclusive. Further work will involve the implantation of enriched nitrogen-15 (about 0.4% relative abundance in nature); in this case a nuclear-reaction examination [by means of the $^{15}N(p,\alpha\gamma)^{12}C$ reaction] will reveal definitively the presence or absence of the implanted nitrogen under the wear scar because the signal from natural nitrogen from the manufacturing process or from subsequent contamination will in effect be attenuated by a factor of about 200.

Scanning electron microscope (SEM) photographs were taken of spots on the wear scars on the ball. Figure 18 shows two such photographs from implanted surfaces (upper pair) and two such photographs from unimplanted surfaces (lower pair). The unimplanted surfaces appear to have substantial craters whereas the dark places on the implanted surfaces appear to be only stains resulting from chemical changes in the lubricant. Additional SEM examinations will be made of unimplanted and implanted wear scars after covering them with a thin (few-hundred-Ångstrom-thick) conductive gold layer. These examinations will allow a better description of any organic polymer layers present on the wear surfaces. (The presence of such layers is indicated by optical microscopy examinations described below.)

A preliminary Ferrographic examination of the wear particles was made at the Foxboro/Trans-Sonics laboratory in a cooperative effort between NRL and Foxboro/Trans-Sonics. These preliminary results tend to confirm the improvement in wear resistance of implanted surfaces and may help to delineate the empirical reason for the improvement in wear resistance. The following preliminary observations were made.

(i) The wear particles from the implanted surfaces were on the average finer than those from the unimplanted surfaces, but exhibited the same morphology.

(ii) There appeared to be fewer wear particles from the implanted surfaces than from the unimplanted surfaces.

(iii) There were more friction polymer particles in the oil from the implanted surfaces than from the unimplanted surfaces. (Friction polymer is polymerized lubricant in the form of flakes or small sheets.)

(iv) There were, in the implanted-surface samples, particles rolled up in friction polymer sheets; but none were found in the unimplanted surface samples. These were like miniature tamales with the wear particles analogous to the minced meat and with the friction polymer analogous to the corn shuck.

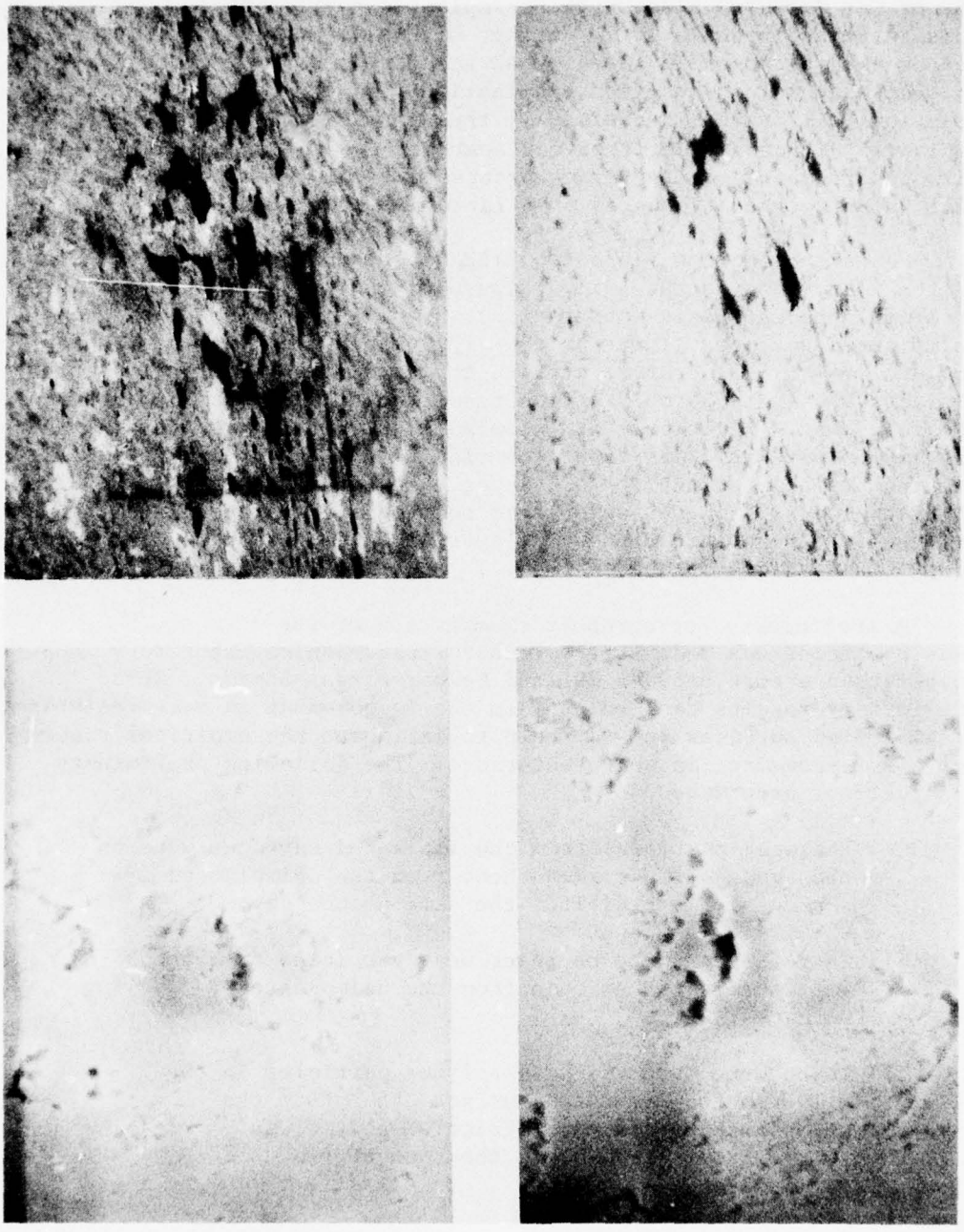


Fig. 18 — Scanning electron microscope pictures (5,000 X magnification) of spots within the wear scars on the ball, comparing implanted region scars (upper pair) and unimplanted region scars (lower pair)

These first two observations concerning the average size and number of particles are consistent with the improvement in wear from the wear measurements. And the two observations concerning the friction polymer might imply the basic reason for the improvement in wear. Thus, it may be that the surface chemistry of the implanted surface is modified in a way that significantly affects the lubricant film between the surfaces, enhancing the production of friction polymer and perhaps affecting the physical characteristics of the polymer (e.g., making it more adhesive and stronger). Such a film would tend to reduce the degree of metal-to-metal contact and hence the wear rate.

The detailed examinations of the wear particles and associated polymers are expected to provide information that will help, along with the information from further wear tests, in the optimization of the implantation parameters for reducing wear of AISI-52100 steel bearings. That is to say, the result of this investigation should be a process for producing a new steel having the bulk properties of AISI-52100 steel but with substantially more wear-resistance surface properties.

N. Modification of Friction by Ion Implantation (W. H. Lucke and R. Bowers*)

To explore the effects of ion implantation on the friction between materials of bearing quality, a plate of AISI-52100 steel about 2 inches square by 1/2 inch thick was implanted to a fluence of 10^{18} N/cm^2 with 80-keV N_2^+ ions (i.e., 40 keV/atom). The implanted region was a strip about one centimeter wide across the plate. In addition, a portion of a 0.5-inch ball bearing was also implanted to a fluence of 10^{18} N/cm^2.

Friction measurements were made with an apparatus designed to measure and record both (i) the normal force between the ball and the plate (in this case, 1 kgm-weight) and (ii) the dragging force experienced by the ball as it was drawn across the plate at a constant velocity. The coefficient of friction at any particular point on the plate was determined from the ratio of simultaneous values picked off the recorder tracings. The experiment was arranged so that on each traversal the ball began its track in an unimplanted region of the plate, was dragged across the implanted region, and ended up on an unimplanted region. In order to compare the effects of the implanted ball with an unimplanted one, it was necessary to reposition the ball in its holder between trials. (Here "trial" refers to a set of repeated traversals of the same track.)

*Chemistry Division, Naval Research Laboratory.

Unlubricated Trials

The first trials were made without lubrication. For the first traversals of each trial the coefficient of friction μ was independent of whether the ball was implanted, and the implanted regions of the plate showed about twice the μ values of the unimplanted regions. This difference was probably due to a contaminant on the unimplanted surface, which had been sputtered off the implanted region, since from the third traversal on, in each trial, the unimplanted μ values were essentially the same as the implanted ones (which did not change significantly).

Lubricated Trials

In an attempt to see what effects ion implantation might have in the presence of lubrication, two trials consisting of 100 traversals were conducted. The lubricant used was USP mineral oil from NPL supply. One trial involved the implanted region of the ball; the other, an unimplanted region. For the initial traversals (1-10) the oil reduced the friction of the unimplanted surface by a factor of about three; and, of the implanted surface by a factor of about six, both for the implanted ball and the unimplanted ball. Thus there was no significant difference between implanted friction and the unimplanted friction (the data showed a lot of scatter). From traversal to traversal the friction of the unimplanted regions remained the same whereas for the implanted regions the friction increased. For the unimplanted ball the increase was by a factor of about 1.6 whereas for the implanted ball it was 1.4. The significance of this difference is marginal.

Wear

An attempt to measure wear was only partially successful. In the case of the ball the diameter of the flat area abraded by traversal of the plate was measured, and from this the depth of material removed could be calculated. The results, however lacked consistency. Attempts were made to measure the depths of the wear grooves in the plate with a Tally-Surf instrument. No useful results were obtained. It is possible that the grooves were so shallow as to be beyond the sensitivity of the instrument, especially since the plate was not flat but wedge shaped.

A peculiarity encountered in the course of this work perhaps deserves mention. It was noted that two very narrow bands, on either side of and immediately adjacent to the implanted region, showed low friction and, as judged by microphotographs, low wear. Since these bands were not observed in subsequent work on Au implanted with various ions, it is possible that they were related to the deformation of the steel surface caused by the increase in volume commonly encountered in implanted materials.

O. Ion Implantation of Au Electrical Contacts (R. Bowers* and W. H. Lucke)

Under the conditions encountered in a Poseidon missile, i.e., the accumulation of volatile compounds in the enclosed atmosphere, a major factor in the production of electrical noise by slip rings results from contamination of the lubricant with ambient impurities which react with it chemically. A possible solution to the problem would be to eliminate the lubricant by implanting the slip rings with a low-friction low-wear material.

Since the slip rings are comprised of gold fingers (or brushes) sliding on gold rings, the actual system could be conveniently imitated by gold coupons (thin strips one centimeter wide by about six centimeters long) as the rings and a gold-plated half-inch-diameter steel ball for sliding contact. Such an arrangement readily fits the available friction measuring apparatus. Five atomic species were implanted at an energy of 80 keV. Three of these (Al, Cr, and Sn) were implanted into coupons only. Two (Cd and Fe) were implanted into both coupons and ball; and two fluences of Cd were used: 10^{16} Cd/cm^2 and 10^{18} Cd/cm^2. The Fe fluence was 10^{16}/cm^2, as was Cr. The Al and Sn fluences were 10^{17}/cm^2.

The results showed that ion implantation, with these species at least, gave no advantage over the unimplanted Au on unimplanted Au, whether implanted Au was in contact with unimplanted Au or with implanted Au.

In the course of investigating possible contamination of the Au plating used, friction measurements were made using a plain (AISI-52100 steel) ball on the implanted area of the coupons. The results in Figure 19 show that generally, after a few initial traversals, the implanted coupons gave lower friction coefficients than the unimplanted areas. For implanted Fe the reduction is a factor of two or more. The significance of this finding is not clear.

P. Ion Implantation in Superconducting Niobium Thin Films (S. Wolf† and J. K. Hirvonen)

Iron ions have been implanted into thin films of superconducting niobium in order to reduce the critical current density of the niobium in a localized area. This region of "weakened" superconductivity is essential to the operation of a type of magnetic field sensor called by the acronym SQUID (Superconducting Quantum Interference Device); this sensor has very high sensitivity at low frequencies (e.g., 10^{-10} gauss at 1 Hz). Multiple implantations of iron at 10 keV and 50 keV

*Chemistry Division, Naval Research Laboratory
†Material Sciences Division, Naval Research Laboratory

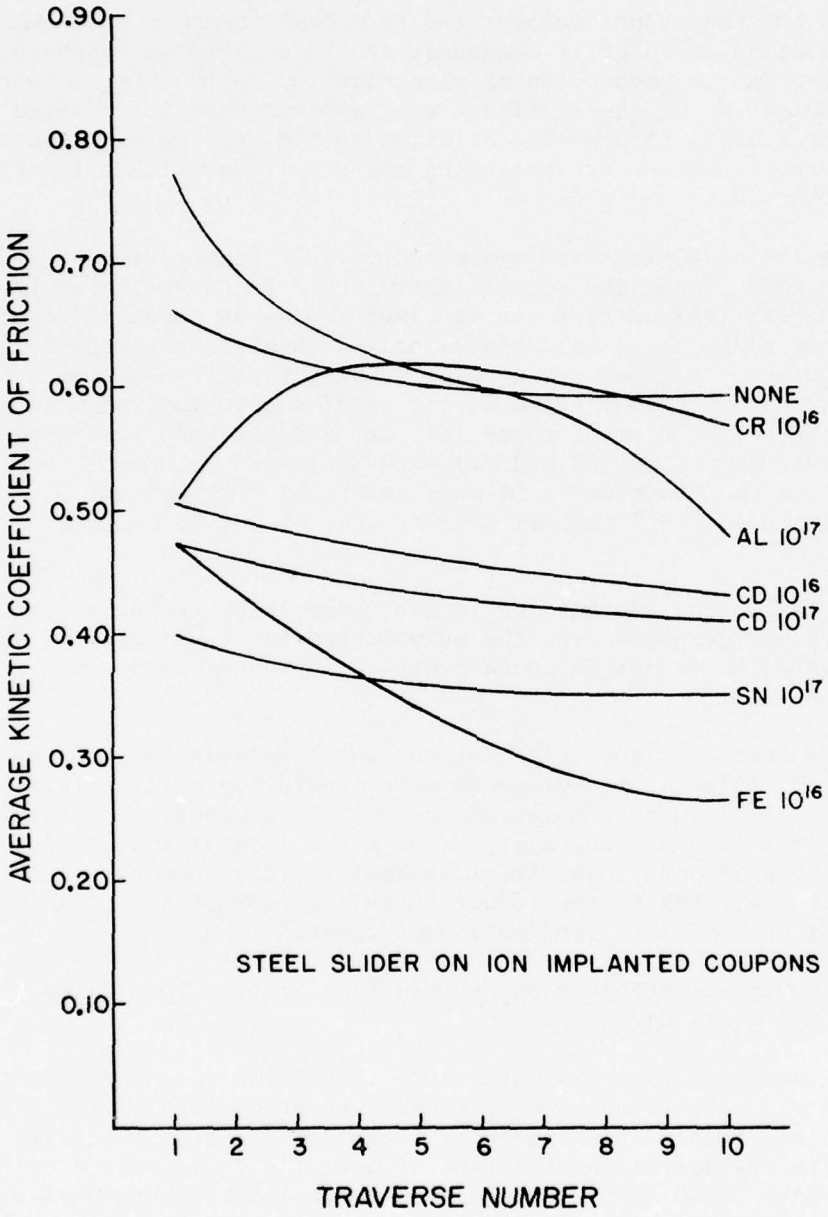


Fig. 19 — Results of kinetic-friction tests for implanted and unimplanted coupons. For the first traversals the similarities of friction coefficients imply a surface contamination; subsequent traversals show the effects of implantation.

to average concentrations from 2 at. % to 15 at. % produce a monotonic decrease in the superconducting transition temperature and critical current behavior of 240-Å niobium films; presumably this effect is due to the radiation damage produced. Iron implantation at 5 at. % to 10 at. % concentration provided a sufficient "weakening" of the implanted area to allow these devices to operate as SQUIDS.

Q. The Application of Pearson Distributions to Implanted Ion Profiles (W. H. Lucke)

With the continued refinement of analyzing techniques, it has become clear that the concentration profile of implanted atoms is not, in general, adequately represented by the standard Gaussian frequency function. Profiles frequently show a pronounced skewness and a long tail. Whereas the Gaussian required the evaluation of only the zeroth, first, and second moments (having zero skewness and a kurtosis of 3), other frequency functions having nonzero skewness and kurtosis values greater than these, require the evaluation of at least the third and fourth moments. Given then that additional information is required, how is it to be incorporated in an analytic expression?

In the late 19th and early 20th century Karl Pearson addressed the problem of describing analytically any skewed distribution in terms of its zeroth through its fourth moments. He assumed that the logarithmic derivative of any such frequency function y could be written:

$$\frac{1}{y}\frac{dy}{dx} = \frac{x - a}{b_o + b_1 x + b_2 x^2} \qquad (1)$$

The constant a gives the x-coordinate of the mode, and the quadratic in the denominator must be well behaved in the regions of interest. The four constants, a, b_o, b_1, and b_2 must now be evaluated in terms of the zeroth through the fourth moments. The variable y must go to zero at both extremes of the region of interest.

Having evaluated the constants in Eq. (1) the next step is to integrate it. It is at once evident that the form of the integral will depend on the nature of the roots of the quadratic. For this reason there is no single expression for y valid for all reasonable values of skewness and kurtosis. To discuss this problem further we introduce a skewness parameter γ_1 defined as the ratio of the third moment to the cube of the standard deviation, and a kurtosis parameter β_2 defined as the ratio of the fourth moment to the fourth power of the standard deviation. The present investigation shows that there is a critical value β_{2c} given by

$$\beta_{2c} = 3\left[\frac{13\gamma_1^2 + 16 + 2(\gamma_1^2 + 4)^{3/2}}{32 - \gamma_1}\right], \qquad (2)$$

which describes the boundary between the region of real roots and that of imaginary ones.

For $\beta_2 > \beta_{2c}$ the roots are imaginary and

$$\ln y = \frac{1}{2b_2} \ln|b_o + bx + b_2x^2| - \frac{A}{\sqrt{B}} \arctan \frac{(2b_2x + b_1)}{\sqrt{B}} ,$$

where

$$A = b_1/b_2 + 2b_1 \text{ and}$$

$$B = 4b_ob_2 - b_1^2 .$$

Pearson refers to this solution as a type-IV distribution.

For $\beta_2 < \beta_{2c}$ the roots are real and

$$\ln y = \frac{1}{2b_2} \ln|b_o + b_1x + b_2x^2| - \frac{1}{2} \frac{A}{\sqrt{-B}} \ln\left|\frac{2b_2x + b_1 - \sqrt{-B}}{2b_2x + b_1 + \sqrt{-B}}\right|$$

(Pearson's type VI).

Whereas for $\beta_2 = \beta_{2c}$

$$\ln y = \frac{1}{2b_2} \ln|b_o + b_1x + b_2x^2| + \frac{A}{2b_2x + b_1}$$

(Pearson's type V).

The normalization factors for types V and VI can be evaluated from the Gamma function. For the type-IV distribution Pearson published a set of tables in the first edition of *Biometrika Tables for Statisticians*, Volume 1, Cambridge University Press (1919).

Fundamentally, the question is whether the lowest five moments of an implanted atom profile can afford an adequate description of that profile. In view of the fact that such a profile represents the end result of many events, each of which occurs according to a rather smoothly varying function of ion energy, we are inclined to think it can. So far as we know, no theoretical investigation of the problem has been undertaken, and experimental evidence is sparse. However it should be mentioned that experimental results of Hofker et al.[1] on boron into silicon over the energy range 30 to 800 keV are extremely well fitted with a type-IV distribution even though β_2 values ranged from 3.6 to 60.

Whether it will be possible to apply the Pearson system generally to all ion-substrate combinations and energy values of interest is not clear.

[1] W. H. Hofker, D. P. Oostheok, N. J. Leoman, and H. A. M. Degrefte, Radiation Effects 24, 223 (1975).

V. SERVICE NOTES

The majority of the Van de Graaff and ion implantation system beam times are used for projects involving direct and substantive scientific participation by Branch personnel in collaboration with non-Branch scientists. Other research projects are performed completely within the Branch. Both of these categories of projects are reported in the preceding section. A small fraction of the beam time is used in irradiations in which Branch personnel perform only minor roles in the scientific aspects of the project; for example, advisory or consultative roles. The present section describes such service irradiations performed during 1975.

A. Charged-particle Damage Study of Wrap-around Junction Solar Cells (G. K. Hubler* and R. L. Statler*)

The wrap-around junction silicon solar cell was recently developed by solar-cell manufacturers to facilitate the fabrication of power packages for space applications and to allow the entire surface area of the solar cell to be coverslipped for improved radiation protection. An important criterion by which solar cells are evaluated for space applications is their electrical performance under charged particle irradiation.

We have irradiated wrap-around junction solar cells (10 Ω-cm, n on p) with 1.0-MeV electrons and 5.0-MeV protons normal to the front surface. The short-circuit current (I_{sc}), open-circuit voltage (V_{oc}) and maximum power (P_{max}) were measured at five temperatures between 10 and 70 °C. Figure 20 shows typical current-voltage characteristics for successive fluences of 5.0-MeV protons and an additional irradiation with 1.0-MeV electrons. These data and the calculated temperature coefficients for I_{sc}, V_{oc}, and P_{max} indicate that wrap-around junction solar cells behave in a similar fashion to standard contact cells but are somewhat more resistant to 1-MeV electron damage (25% loss in P_{max} occurs at 6×10^{14} e/cm^2 for standard contact cells, 8.4×10^{14} e/cm^2 for wrap-around junction cells). In addition, it is demonstrated that sequential applications of proton plus electron, or electron plus proton irradiations to identical fluences cause equivalent degradation of all solar cell output parameters.

A new approach to the first order short-circuit current calculations is employed which adequately predicts the loss of current with increasing particle fluence for 5-MeV protons incident normal to either the front or back solar-cell surface. In this method, the collection of minority carriers at the junction is treated as the probability of transmission of carriers through a solar cell that is divided into a large number of parallel slabs. In this way the effects of a non-uniform minority carrier diffusion length throughout the silicon depth

*Radiation Technology Division, Naval Research Laboratory

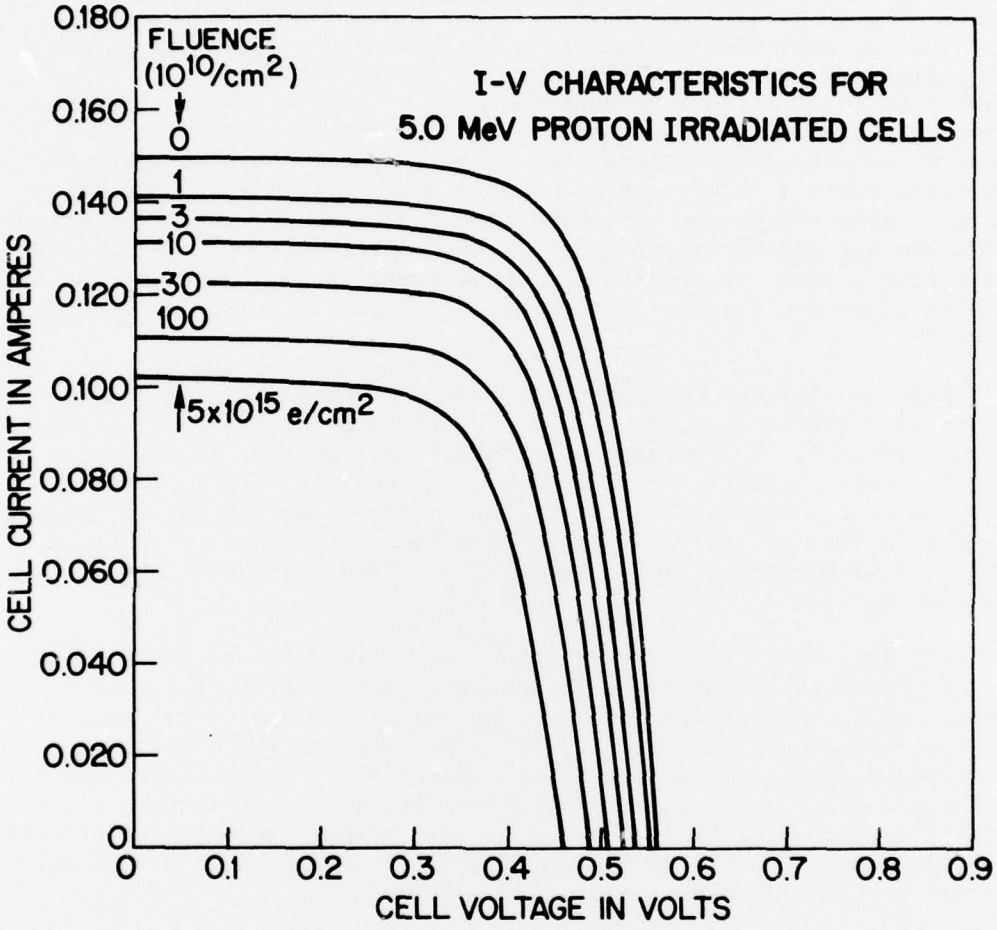


Fig. 20 — Typical I-V characteristics for successive fluences of 5-MeV protons incident normal to the front surface and an additional irradiation with 1.0-MeV electrons. The I-V curves are for AMO illumination and a cell temperature of 25°C.

can be properly accounted for under the assumption that the number of recombination centers is directly proportional to the energy deposited in damage-producing collisions. The energy-deposition program E-DEP-1[1] is used to model the proton damage distribution in Si.

B. Ion Implantation of Cu Laser Mirrors (G. K. Hubler*)

The ion implantation technique has been applied for the purpose of inhibiting corrosion of high-purity copper laser mirrors. High-purity Cu laser mirrors possess the best available damage threshold when subjected to high-intensity 1- to 10.6-μm laser and for this reason would be good material for laser mirrors. However, pure Cu oxidizes rapidly in air and develops a surface film which rapidly deteriorates the damage threshold of the mirror. Protective coatings have similar undesirable effects. The Radiation Technology Division is investigating the possibility of passivating the Cu surface by ion implantation and thereby increasing the usable lifetimes of OFHC Cu mirrors.

A 10-cm-diameter Cu mirror has been implanted in several 1-cm^2 areas with the ions He, N, Al, Ne, and Cr to concentrations of several atomic percent. The purpose of this initial work was to determine whether three criteria could be met which would result in improved laser mirror performance. The criteria are (1) to inhibit the tarnishing of the Cu surface, (2) to maintain the high reflectance of pure Cu at infrared wavelengths, (3) to maintain the high damage threshold of pure Cu mirrors.

All implanted areas in the above experiments inhibited the formation of a surface corrosion film, He being the most effective. Nuclear reactions, Rutherford backscattering, and ion-induced x-ray analyses of the corrosion films after a 70-day exposure to the laboratory atmosphere revealed that the films consisted of roughly equal amounts of oxygen and chlorine (1000 Å thick on the unimplanted area). The origin of the chlorine is unknown at this time. The measured reduction in film growth for the He implanted area with respect to unimplanted Cu was better than a factor of 5.

Specular-reflectance measurements on the implanted areas (at 10.6-μm wavelength) prior to formation of a corrosion film showed that for He and low fluences of Al the relative reflectance (R) between pure Cu and the implanted areas was unchanged. Reductions in R were measured for N, Ne, Cr, and high-fluence Al. The reduction in R was correlated with the product of fluence and sputtering coefficient (e.g., amount of copper removed by sputtering). Because of measurement difficulties due to the large size of the Cu mirror, the accuracy of these reflectance measurements was only $\pm$ 1%. These initial results were promising since criteria (1) and (2) appeared to be satisfied.

---

[1] I. Manning and G. P. Mueller, Computer Phys. Comm., 7, 85 (1974).
*Radiation Technology Division, Naval Research Laboratory.

Several commercial 2.5-cm diameter laser mirrors have been ordered in order to extend these measurements. Damage-threshold measurements will be performed on these mirrors after ion implantation to examine the third criterion listed above.

More accurate specular reflectance measurements are underway on 1.25-cm diameter Cu buttons polished to a mirror finish. The ions He, Be, B, Mg, and Al will be implanted; and the effects of these ions on corrosion and reflectance, studied. Preliminary results for He implanted into these Cu samples are quite encouraging ($R^{He}_{Cu}/R_{Cu} = 0.999 \pm 0.002$).

C. Depth Profiling by Nuclear Resonance Method* (K. L. Dunning†)

During the past year, many measurements have been made on SiO_2-Si test structures containing sodium (deliberately introduced) in order to investigate the migration of sodium at elevated temperatures, in radiation environments, and in electric fields. A few measurements have been made on test structures consisting of a silicon film on sapphire (Al_2O_3) in order to investigate the migration of aluminum at elevated temperatures.

D. Particle-channeling Investigation of Silicon Lattice Reordering (H. D. Dietrich** and J. K. Hirvonen)

Silicon implanted with high doses of aluminum ($>10^{15}$ Al atoms/cm^2) shows anomalous redistribution of the implanted aluminum when subsequently annealed to high temperatures ($\approx$800 °C). Particle-channeling measurements were performed to check for a correlation between this redistribution and the reordering of the silicon lattice.

The channeling measurements showed that a 70-keV Al implantation (2×10^{15} Al atoms/cm^2) produced a highly damaged buried layer which annealed from both sides at annealing temperatures of 450 °C and 475 °C (30 min.). A 500-°C annealing treatment moved most (>90%) of the long-range lattice disorder and left only a small amount of disorder as seen by de-channeling of the incident channeled 2-MeV He ions.

---

*This work was done for the Electronics Technology Division and was partially supported with DNA Subtask Z99QAXTA007 funds.

†Radiation Technology Division, Naval Research Laboratory.

**Electronics Technology Division, Naval Research Laboratory.

E. Nuclear Reaction Analysis of SiON Thin Films (W. A. Schmidt* and J. K. Hirvonen)

SiON is used as a dielectric film on electronic devices made from InSb. The relative ratio of oxygen and nitrogen in these films was determined by means of nuclear reaction analyses in order to correlate these data with the parameters for growing the SiON films.

The analyses for ^{16}O and ^{14}N were simultaneously performed by detecting particles from both the (d,p) and (d,α) reactions produced by a 900-keV incident deuteron beam. The reaction products were detected in a conventional solid-state detector covered with a thin nickel foil to absorb the elastically scattered deuterons.

The films contained relatively small amounts of nitrogen (all less than about one at. %) whose concentration depended on the growth parameters.

F. Detection of Cl in SiO_2-Si Samples by Rutherford Backscattering (P. R. Reid* and J. K. Hirvonen)

Chlorine plays an important but yet not fully understood role in reducing the detrimental effects of sodium in silicon dioxide-silicon electronic devices.

The object of this investigation was to determine the amount of chlorine present and its location relative to the SiO_2-Si interface for oxides prepared with different concentrations of chlorine (HCl) present during the oxide growth.

A magnetic spectrometer was used to detect the backscattered helium ions (3.1 MeV incident energy) in order to enhance the sensitivity to chlorine (see section IV I for a discussion of this factor).

The experiments showed the chlorine present (from about 0.1 to 1.0 x 10^{15} Cl atoms/cm^2) to be most concentrated at the Si-SiO_2 interface.

*Electronics Technology Division, Naval Research Laboratory.

VI. PUBLICATIONS AND TECHNICAL TALKS

A. Publications in Archival Journals

W. H. Lucke J. Comas* G. K. Hubler* K. L. Dunning*	"Effects of Annealing on Profiles of Aluminum Implanted in Silicon Carbide," J. Appl. Phys. 46, 994 (1975).
D. J. Nagel* A. R. Knudson P. G. Burkhalter*	"Ion-Excited XUV Radiation from Solid Targets," J. Phys. B: Atom. Molec. Phys. 8, 2779 (1975).
J. E. Westmoreland J. A. Sprague* F. A. Smidt, Jr.* P. R. Malmberg	"Flux Dependence of Void Nucleation and Void Growth in 2.8-MeV Nickel-Ion-Irradiated Nickel," JVST 12, 511 (1975).
J. E. Westmoreland J. A. Sprague* F. A. Smidt, Jr.* P. R. Malmberg	"Dose Rate Effects in Nickel-Ion-Irradiated Nickel," Radiation Effects 26, 1 (1975).

B. NRL Formal Reports and NRL Memorandum Reports

Ion Beam Applications Branch Staff, edited by J. W. Butler	"NRL Van de Graaff Operation 1 January - 31 December 1974," NRL Memo Report 3078, July 1975.
G. P. Mueller* J. E. Westmoreland	"Modification of E-DEP-1 to Run for High Energy Helium Ions in Nickel and Type 316 Stainless Steel," NRL Memo Report 3019, March 1975.
J. A. Sprague* F. A. Smidt, Jr.* J. E. Westmoreland P. R. Malmberg	"Fluence Dependence of Ion Damage in Nickel," in Irradiation Effects on Reactor Structural Materials, Semiannual Progress Report, 1 August - 31 January 1975, L. E. Steele, Editor, NRL Memo Report 3010, February 1975.

*Non-Branch authors are identified alphabetically on page 71.

J. A. Sprague* J. E. Westmoreland P. R. Malmberg F. A. Smidt, Jr.*	"The Fluence Dependence of Nickel Ion Damage in Nickel," in Cooperative Radiation Effects Semiannual Progress Report, 1 May - 31 October 1974, L. E. Steele and E. A. Wolicki, Editors, NRL Memo Report 2998, March 1975.
J. E. Westmoreland J. A. Sprague* F. A. Smidt, Jr.* P. R. Malmberg	"Dose Rate Effects in Nickel-Ion-Irradiated Nickel," in Cooperative Radiation Effects Semiannual Progress Report, 1 May - 31 October 1974, L. E. Steele and E. A. Wolicki, Editors, NRL Memo Report 2998, March 1975.
F. A. Smidt, Jr.* J. A. Sprague* J. E. Westmoreland P. R. Malmberg	"Swelling in Dilute Binary Nickel Alloys," in Cooperative Radiation Effects Semiannual Progress Report, 1 May - 31 October 1974, L. E. Steele and E. A. Wolicki, Editors, NRL Memo Report 2998, March 1975.
L. G. Kirchner* F. A. Smidt, Jr.* G. L. Kulcinski* J. A. Sprague* J. E. Westmoreland P. R. Malmberg	"Ion Damage in Solid Solution and Precipitation Hardened Ni-Al Alloys," in Cooperative Radiation Effects Simulation Program, Semiannual Progress Report, 1 November 1974 - 30 April 1975, L. E. Steele and E. A. Wolicki, Editors, NRL Memo Report 3114, August 1975.
J. E. Westmoreland J. A. Sprague* F. A. Smidt, Jr.* P. R. Malmberg	"Dose Rate Effects on Precipitate Stability," in Cooperative Radiation Effects Simulation Program, Semiannual Progress Report, 1 November 1974 - 30 April 1975, L. E. Steele and E. A. Wolicki, Editors, NRL Memo Report 3114, August 1975.
F. A. Smidt, Jr.* P. R. Malmberg J. A. Sprague* J. E. Westmoreland	"Swelling in Dilute Binary Nickel Alloys," in Irradiation Effects on Reactor Structural Materials Semiannual Progress Report, 1 February - 31 July 1975, L. E. Steele, Editor, NRL Memo Report 3110, August 1975.

*Non-Branch authors are identified alphabetically on page 71.

C. Talks Presented at Scientific Meetings[†]

J. W. Butler	"Materials Modification and Analysis," Nuclear Physics Subelement Review, 3 April 1975.
K. W. Hill A. R. Knudson	"Non-Binomial Distribution of Kα X-Ray Satellite Intensities," American Physical Society, Washington, DC, 28 April - 1 May 1975.
J. W. Butler	"Radiation Vulnerability of Satellites," Captain Pope and others, PME-106, NAVELEX, 7 July 1975.
J. W. Butler	"Ion Implantation and Wear," Meeting of the Materials Research Council, Scripps Elementary School, La Jolla, CA, 15 July 1975.
J. C. Ritter* J. W. Butler	"The Navy's Needs for a Satellite Nuclear Survivability Group," Captain Darcy and others, PME-106, NAVELEX, 12 August 1975.
J. W. Butler	"The Treatment of Energy-Loss Fluctuations in Surface Layer Analysis by Ion Beams," International Conference on Ion Beam Surface Layer Analysis, Karlsruhe, W. Germany, September 1975.
J. K. Hirvonen G. K. Hubler*	"Application of a High Resolution Magnetic Spectrometer to Near-Surface Materials Analysis," International Conference on Ion Beam Surface Layer Analysis, Karlsruhe, W. Germany, September 1975.
K. W. Hill A. R. Knudson	"Non-Binomial Distributions of Satellite Intensity in Kα X-Ray Spectra," Conference on Atomic Collisions in Solids, Amsterdam, the Netherlands, September 1975.

[†]For multiple-author papers, the name of the speaker is underlined.
*Non-Branch authors are identified alphabetically on page 71.

J. Ziegler*	"Computer Analysis of Nuclear Back-
R. Lever*	scattering," International Conference on
J. K. Hirvonen	Ion Beam Surface Layer Analysis, Karlsruhe, W. Germany, September 1975.
J. W. Butler	"Ion Implantation and Wear," ONR-NRL Tribology Workshop, Washington, DC, 14-16 October 1975.
J. K. Hirvonen	"Rutherford Backscattering for Solid State Physics Investigation," University of Delaware, Newark, DE, 7 October 1975.

D. Miscellaneous Reports

J. W. Butler	"(p,γ) Reactions," Excitation Functions for Charged Particle Induced Reactions in Light Elements at Low Projectile Energies, ed. by J. Lorenzen and D. Brune, STI/DOC-10/156, Aktiebologet Atomenergi, Studsvik, Nyköping, Sweden, p. 459, 1974.
J. A. Sprague* F. A. Smidt, Jr.* J. E. Westmoreland P. R. Malmberg	"Void Formation in Nickel-Ion-Irradiated Nickel," Proceedings of the European Conference on Irradiation Behavior of Fuel Cladding and Core Component Materials, Gesellshaft für Kernforschung mbH., Karlsruhe, Germany, 3-5 December 1974, p. 37, December 1974.
F. A. Smidt, Jr.* J. A. Sprague* J. E. Westmoreland P. R. Malmberg	"The Influence of Minor Alloy Additions on Swelling," Proceedings of the European Conference on Irradiation Behavior of Fuel Cladding and Core Component Materials, Gesellshaft für Kernforschung mbH., Karlsruhe, Germany, 3-5 December 1974, p. 81, December 1974.

*Non-Branch authors are identified alphabetically on page 71.

J. E. Westmoreland J. A. Sprague* F. A. Smidt, Jr.* P. R. Malmberg	"Flux Dependence of Void Nucleation and Void Growth in 2.8-MeV Nickel-Ion-Irradiated Nickel," Proceedings of the Symposium on the Physics of Irradiation-Produced Voids, Harwell Atomic Energy Research Establishment, England, 9-11 September 1974, AERE-R7934, p. 268, January 1975.
J. A. Sprague* F. A. Smidt, Jr.* J. E. Westmoreland P. R. Malmberg	"The Determination of Void Formation Parameters in Metals by Heavy Ion Irradiation," Proceedings of the Symposium on the Physics of Irradiation-Produced Voids, Harwell Atomic Energy Research Establishment, England, 9-11 September 1974, AERE-R7934, p. 263, January 1975.
J. E. Westmoreland J. A. Sprague*	"Physics of Irradiation Produced Voids," European Scientific Notes 29-1, (ONR) London, 31 January 1975.
J. E. Westmoreland P. R. Malmberg J. A. Sprague* F. A. Smidt, Jr.*	"Dose Rate Effects in Nickel-Ion-Irradiated Nickel," Report of NRL Progress, February, 1975, p. 45-46.
G. K. Hubler* P. R. Malmberg J. Comas*	"1.2 MeV Al Ion Implantation into SiC," Report of NRL Progress, April 1975, p. 37.
J. A. Sprague* F. A. Smidt, Jr.* J. E. Westmoreland P. R. Malmberg	"Fluence Dependence of Swelling in Ion-Irradiated Nickel," Report of NRL Progress, May 1975, p. 19.
J. W. Butler D. H. Phillips* J. C. Ritter*	"Test Procedure for FLTSATCOM Oven Controlled Crystal Oscillator," Memo 6670-32:JWB/DHP/JCR:ghm of 2 June 1975.
F. A. Smidt, Jr.* J. A. Sprague* J. E. Westmoreland P. R. Malmberg	"Effects of Alloy Additions on Swelling in Nickel," Report of NRL Progress, August 1975, p. 32.

*Non-Branch authors are identified alphabetically on page 71.

F. A. Smidt, Jr.*
L. G. Kirchner*
J. A. Sprague*
J. E. Westmoreland
P. R. Malmberg

"The Stability of Ni_3Al Precipitates Under Heavy Ion Irradiation," Report of NRL Progress, November 1975, p. 17-19.

A. R. Knudson

"High-Resolution Measurements of X Rays from Ion-Atom Collisions, Proceedings of the 3rd Conference on Applications of Small Accelerators, Denton, TX, 21-23 October 1974, J. Duggan and I. Morgan, editors, Vol. I, p. 374, 1975.

D. J. Nagel*
A. R. Knudson
P. G. Burkhalter*

"Ion Excited XUV Radiation Vacuum-Ultraviolet Radiation Physics," Hamburg, W. Germany, 22-26 July 1974, Edited by E. Koch, R. Haensel, and C. Kunz, Pergamon, 1975.

*Non-Branch authors are identified alphabetically on page 71.

Non-Branch Authors*

P. G. Burkhalter, X-Ray Optics Branch, Material Sciences Division, Naval Research Laboratory

J. Comas, Solid State Devices Branch, Electronics Technology Division, Naval Research Laboratory

K. L. Dunning, Consultant, Radiation Technology Division, Naval Research Laboratory

G. K. Hubler, Radiation Effects Branch, Radiation Technology Division, Naval Research Laboratory

L. G. Kirchner, Nuclear Engineering Department, University of Wisconsin, Madison, WI

G. L. Kulcinski, Nuclear Engineering Department, University of Wisconsin, Madison, WI

R. Lever, Thomas J. Watson Research Center, IBM, Yorktown Heights, NY

I. Manning, Radiation Theory Branch, Radiation Technology Division, Naval Research Laboratory

G. P. Mueller, Radiation Theory Branch, Radiation Technology Division, Naval Research Laboratory

D. J. Nagel, X-Ray Optics Branch, Material Sciences Division, Naval Research Laboratory

D. H. Phillips, Systems Integration and Instrumentation Branch, Communications Sciences Division, Naval Research Laboratory

J. C. Ritter, Electron Radiations Branch, Radiation Technology Division, Naval Research Laboratory

M. Rosen, Radiation Theory Branch, Radiation Technology Division, Naval Research Laboratory

F. A. Smidt, Jr., Thermostructural Materials Branch, Engineering Materials Division, Naval Research Laboratory

J. A. Sprague, Thermostructural Materials Branch, Engineering Materials Division, Naval Research Laboratory

J. Ziegler, Thomas J. Watson Research Center, IBM, Yorktown Heights, NY

*Non-Branch authors are identified alphabetically on this page.